Nanoscale Advances

Accepted Manuscript

This article can be cited before page numbers have been issued, to do this please use: P. Shangpliang, S. S. Joshi, S. D. Kulkarni and K. S. Choudhari, *Nanoscale Adv.*, 2026, DOI: 10.1039/D6NA00239K.

ROYAL SOCIETY OF CHEMISTRY

rsc.li/nanoscale-advances

DOI: 10.1039/D6NA00239K

Room Temperature VOC Detection Using Light-Driven Metal Oxide Heterojunctions: Principles, Challenges, and Prospects

Phibakordor Shangpliang [a], Suraj Sunil Joshi [a], Suresh D Kulkarni [a], and K.S. Choudhari*[a]

[a] *Manipal Institute of Applied Physics, Manipal Academy of Higher Education, Manipal, Karnataka 576104, India*

**Corresponding author: choudhari.ks@manipal.edu*

Volatile organic compounds (VOCs) are a very important class of pollutants and biomarkers of diseases, which require the development of highly sensitive sensors. This review article critically discusses the recent advances in the development of semiconductor metal oxide (SMO) heterojunction-based chemiresistive sensors for VOC detection, particularly with the use of light-activated sensing mechanisms to improve the performance parameters of sensitivity, selectivity, response time, and stability. The basic sensing mechanisms, such as band engineering, charge transfer processes, room-temperature sensing, and heterojunction designs, are comprehensively reviewed to understand their role in gas adsorption and sensing response modulation. This review article also discusses the conventional limitations of pristine SMO sensors, such as temperature limitations and drift effects, and how the use of heterojunctions along with ultraviolet and visible light activation can overcome these limitations and improve the performance of gas sensors. The integration of these sensors in smart devices and Internet of Things (IoT) applications is reviewed, with special emphasis on wearable and packaging devices for environmental and food quality monitoring. Moreover, the application potential of these sensor systems in medical diagnostics is highlighted by examples of VOC biomarkers for diabetes and lung cancer. The critical challenges in the current research are also pointed out, including the need for improved stability in different humidity conditions, selectivity, and scalable fabrication techniques. The review concludes by outlining the future directions, including hybrid materials, flexible electronics, and artificial intelligence-assisted, IoT-enabled sensor development providing a forward-looking roadmap for intelligent and advanced VOC sensing technologies towards real-world applications. This thorough review is intended to provide a basis for future innovations in materials-based sensor technologies, in line with the emerging challenges in society.

Keywords: Room-Temperature VOC Sensing, Light-Activated Gas Sensors, Metal Oxide Heterojunctions, Chemiresistive Sensors, UV/Visible Light Activation, Volatile Organic Compound, Artificial Intelligence

1. Introduction

Environmental pollution has become a challenge to the global community due to the increased growth of technological and industrial activities. The constant growth of technological and

View Article Online
DOI: 10.1039/D6NA00239K

industrial systems to meet industrial demands poses a threat to the health of human beings and the environment.[1] Among the many forms of pollution, air pollution is the most widespread environmental problem that poses a threat to the health of human beings.[2] With a composition of toxic, flammable, and explosive gas pollutants such as carbon monoxide (CO), hydrogen sulphide (H_2S), ammonia (NH_3), nitrogen dioxide (NO_2), methane (CH_4), propane (C_3H_8), hydrogen (H_2), and volatile organic compounds (VOCs) such as acetone, benzene, isopropanol, ethanol, and methanol, global warming and climate change has enhanced immaculately, posing numerous health hazards.[3–5] Air pollution has been identified by the World Health Organization (WHO) as one of several factors that worsen respiratory diseases (e.g., asthma) and increase the prevalence of pneumonia and other infections in children; it is also a cause of the death rate from diseases of the heart, including stroke, chronic respiratory diseases, and several different types of cancer. In 2016, indoor and outdoor air pollution caused approximately seven million deaths worldwide, which is the fourth leading cause of global mortality.[5,2,6]

VOCs are a large class of carbon-based substances that are very volatile at ambient temperature. VOCs are easily vapourized from a variety of sources and are detrimental to human health, the environment and the industry. They are released from both anthropogenic (i.e., human-created) sources (e.g., motor vehicles, industrial solvents, paint and fuel) and from non-anthropogenic (i.e., natural) sources (e.g., volatile emissions from plants). Common VOC types include aromatic hydrocarbons (e.g., benzene, toluene, xylene), aldehydes (e.g., formaldehyde), ketones (e.g., acetone), alcohols, and halogenated compounds, each exhibiting unique characteristics with regard to volatility and reactivity that challenge selective detection. The International Agency for Research on Cancer (IARC) has classified benzene and formaldehyde as Group 1 carcinogens.[6,7]

VOCs contribute to tropospheric ozone formation, photochemical smog, and secondary organic aerosols, exacerbating climate change and air pollution globally.[4,6,8] The concentration of VOCs indoors can be ten times higher than outside, and different VOCs may be the cause of different health problems both acute (e.g., eye and mucous membrane irritation) and chronic (e.g., asthma and cancer) diseases as well as various environmental issues (e.g., ozone and particulate formation).[8]

In industry, VOC analysis is critical for process safety, leak detection in petrochemical industries, and regulatory requirements such as the U.S. EPA's National Emission Standards,

View Article Online
DOI: 10.1039/D6NA00239K

thus highlighting the importance of VOC analysis in workplace safety, food spoilage analysis, and breath analysis for non-invasive disease diagnosis.[9]

Conventional VOC sensing techniques, such as gas chromatography-mass spectrometry (GC-MS) and photoionization detectors, have high accuracy and detection limits as low as parts-per-billion (ppb) but are plagued by significant disadvantages, including high capital costs, long analysis times (typically >30 minutes per sample), bulky hindering portability, and the need for highly trained personnel for operation and analysis.[10] These limitations hinder real-time, on-site monitoring, which is essential for dynamic scenarios such as urban air quality assessment, industrial leak detection, and wearable health devices, where rapid response and recovery times of under one minute, as well as functionality in humid atmospheric conditions are important. Electrochemical and optical sensors offer partial alternatives but are often deficient in sensitivity, selectivity in the presence of interferents, or environmental stability.[114]

Semiconductor metal oxide (SMO) chemiresistive sensors appear as a better alternative, which allow resistance monitoring through VOC adsorption-driven charge depletion or accumulation in surface sites, allowing for miniaturized, low-power sensors with sensitivities comparable to those of GC-MS systems at a fraction of the cost.[12] However, pristine SMO materials, such as SnO_2 and ZnO, face limitations, including baseline drift, poor selectivity due to broad baseline responses to humidity and interferents, higher operating temperatures (>200 °C), which risks high energy consumption and safety concerns.[13,14,15] Heterojunction engineering, which involves the use of type-II or Schottky interfaces between different SMO phases (e.g., SnO_2/ZnO, WO_3/In_2O_3), overcomes these challenges by facilitating efficient charge separation, increased depletion layer thickness, and Fermi level tuning, resulting in sensitivity enhancements of 10–100 times and improved selectivity.[16]

Light activation also improves the performance of SMO heterojunctions by photo-excitation of electron-hole pairs, desorbing oxygen species to renew active sites, lowering working temperatures to room temperature, and increasing modulation depths under UV or visible illumination by bandgap engineering with dopants or plasmonics.[17] This review offers a comprehensive overview of light-activated semiconductor metal oxide (SMO) heterojunctions for volatile organic compound (VOC) detection. It includes the basic concepts of chemiresistive sensing, the natural limitations of pristine SMOs, and various heterojunction configurations such as p-n, n-n, and Schottky junctions, as well as their band structures and charge transfer mechanisms. UV and visible light activation methods, important performance

View Article Online
DOI: 10.1039/D6NA00239K

metrics, and system-level integration with IoT-based wearables and smart sensing systems are also considered. Through the compilation of recent advances until 2025, the review indicates the existing limitations in scalable device fabrication and intelligent AI-based signal processing and offers a long-term vision for the future of selective VOC detection in forensic science, medicine, and environmental conservation. The following sections provide a detailed description of SMO basics, heterojunction-mediated sensing mechanisms, implementation aspects, and future research trends, providing a basis for the subsequent discussion on VOC background, sources, types, and significance.

1.1. Background on VOCs (Sources, Types, Impacts) and their Significance

Volatile organic compounds are defined as low molecular weight, carbon-based organic compounds that have elevated vapor pressure, low water solubility, boiling points in the range 50 ºC and 250 ºC and an atmospheric pressure of 101.3 kPa.[18] As a result, they can easily vaporize in ambient environments. VOCs contain a wide array of chemical classes, ranging from aliphatic and aromatic hydrocarbons, aldehydes, ketones, esters, ethers, acids, and alcohols. Organic compounds attaining molecular weights as high as 150 g/mol are generally present in the gaseous state, and compounds attaining molecular weights within the range of 150-225 g/mol are classified as semi-volatile or non-volatile. They have restricted half-life and can be readily modified by environmental factors.[19,20] Table 1 represents the essential VOCs classified in different categories, along with their chemical and physical characteristics.

1.1.1. Types of VOCs

Based on their boiling points and volatility, VOCs are classified as (i) Very volatile organic compounds (ii) Volatile organic compounds and (iii) Semi-volatile organic compounds.[18]

- **Very volatile organic compounds (VVOCs):** Includes compounds with a boiling point ≤100 °C. They are toxic at minute concentrations, with compounds ranging from propane and butane to methyl chloride and chloroform. They originate from both natural sources, for example, acetic acid emitted by coniferous and deciduous trees, and human activities, including fuel combustion, cooking, and the use of household products like cleaners, paints, and deodorants.

View Article Online
DOI: 10.1039/D6NA00239K

Table 1. Physicochemical Properties and Occupational Exposure Limits of Representative VOCs

Group	VOC	Formula	M (g/mol)	Boiling Point (°C)	Vapor Pressure (mm Hg)	Toxicity	OSHA PEL*	NIOSH REL@ Upto 10 hrs TWA
C1	Formaldehyde	HCHO	30	-21	>760	Cat.3 Carcinogen	0.75 ppm (8 hr TWA)	0.016 ppm (8 hr)
	Methanol	CH_3OH	32	64.6	96	Toxic	200 ppm (8 hr TWA)	200 ppm (10hr)
	Chloromethane	CH_3Cl	50.5	-24.1	3800	Cat.3 Carcinogen	100 ppm	NA
C2	Ethanol	C_2H_5OH	46.1	78.3	44	Unclassified	1000 ppm (8 hr)	1000 ppm (10 hr)
	Acetaldehyde	CH_3CHO	44.1	20.8	740	Cat.3 Carcinogen	200 (8 hr TWA)	NA
	Acetic acid	CH_3COOH	60.1	117.9	11	Harmful	10 ppm	10ppm
C3	Propane	C_3H_8	44.1	-42.1	6384 at 70°F	Unclassified	1000 ppm (8 hr)	1000 ppm (10 hr)
	1-Propanol	$CH_3(CH_2)_2OH$	60.1	97.2	40 at 36.4 °C	Harmful	200 ppm (10 hr)	200 ppm (10 hr)
	2-Propanol	$CH_3CH(OH)CH_3$	60.1	82.3	43 at 23.8 °C	Unclassified	400 ppm	400 ppm

	Propanoic acid	C_2H_5COOH	74.1	141.1	3	Harmful	NA	10 ppm (10 hr)
C4	n-Butane	C_4H_{10}	58.1	-0.5	1558	Unclassified	NA	800 ppm (10 hr)
	1,3-Butadiene	$CH_2CHCHCH_2$	54.1	-4.4	1824	Potential occupational carcinogen	1 ppm	NA
C5	n-Pentane	C_5H_{12}	72.2	36.1	420	Unclassified	1000 ppm (8 hr)	120 ppm (10 hr)
	Cyclopentane	C_5H_{10}	70.1	49.2	400 at 88°F	Unclassified	NA	600 ppm
C6	N-Hexane	C_6H_{14}	86.2	69	124	Harmful	500 (8 hr)	50 ppm (10 hr)
	N butylamine	$CH_3(CH_2)_3NH_2$	73.139	77	72	Unclassified	5 ppm	300 ppm

***OSHA** – Occupation Safety and Health Administration; **PEL** – Permissible Exposure Limit; **TWA** – Time Weighted Average

@ **NIOSH** – National Institute for Occupational Safety and Health; **REL** – Recommended Exposure Limit

NA - Not Available

https://www.osha.gov/annotated-pels/table-z-1

- **Volatile organic compounds (VOCs)**: This category covers compounds with boiling point 100-260 °C. Major constituents often stem from household products and industrial solvents such as formaldehyde, acetone, and toluene.
- **Semi-volatile organic compounds (SVOCs):** These include compounds with higher boiling points, typically in the range 260-400 °C and include substance like phthalates, and pesticides like DDT.[18] SVOCs generally have greater molecular weights and lower volatility compared to VVOCs and VOCs.

1.1.2. Sources of VOCs

VOCs originate from both natural and anthropogenic sources shown in Fig. 1. Biogenic emissions from vegetation, particularly isoprene and monoterpenes, constitute ~80% of the total global VOC flux.[21]

View Article Online
DOI: 10.1039/D6NA00239K

a) Anthropogenic:

Anthropogenic sources dominate urban environments and include: (a) Outdoor sources: Industrial solvents (paints, adhesives), fossil fuel combustion, vehicle exhausts, biomass burning, and waste treatment, contributing ~150 Tg/year globally, and (b) Indoor sources: Building materials, furnishings, cleaning products, cooking, and personal care items. Indoor VOC concentrations typically exceed outdoor levels by 2.5 times due to limited ventilation and off-gassing.[22,23] Microbial volatile organic compounds (mVOCs) from dampness and poor ventilation contribute to sick building syndrome, exacerbating indoor air quality issues.[24,25] These source profiles create complex, multi-component VOC mixtures that challenge sensor sensitivity and selectivity. This complexity is particularly concerning for indoor exposure, where people spend ~90% of their time (in offices, schools, and residences), resulting in higher cumulative doses despite lower concentrations.[18] Yet, natural sources contribute the dominant global VOC flux, primarily through biogenic processes.[26]

b) Natural:

Terrestrial vegetation generates ~90% of the global VOC, approaching 1150 Tg/year. Major contributors are Isoprene 62% (~600 Tg/year), and monoterpenes, (22%) (~200 Tg/year), through stomatal and cuticular release mechanisms. [27,28] Forests account for ~70% of the terrestrial biogenic emissions, with temperature and photochemical dependences. The key natural contributors include:

- Vegetation: Isoprene from broadleaf trees, monoterpenes from conifers (~90% biogenic total).[29]
- Wildfires: Aromatic VOCs, furans (~20-50 Tg/year globally).[30]
- Microbial VOCs (mVOCs): 1-octen-3-ol, geosmin from fungi/bacteria in soil/damp environments (~5-10 Tg/year).[25]
- Oceanic/Animal: Minor contributions from marine algae, methane oxidation.[21, 31]

These chemically diverse biogenic VOCs pose significant baseline interference challenges for anthropogenic VOC sensors, particularly in rural/forested regions. Understanding VOC impacts is crucial for sensor design, as detailed below. Minor health impacts of VOCs include eye/skin irritation, headaches and chronic effects, including neurotoxicity, reproductive toxicity, and carcinogenicity.[32] Benzene, classified as a Group 1 carcinogen by the IARC, induces DNA double-strand breaks and chromosomal aberrations, leading to acute myeloid leukemia (AML) through CYP2E1-mediated metabolism to benzene oxide.[33,34] Toluene causes

central nervous system depression and ototoxicity at chronic exposures >50 ppm, with co-exposure studies showing toluene inhibits benzene metabolism, potentially modulating leukemia risk.[35] Formaldehyde (Group 1 IARC carcinogen) causes nasopharyngeal cancer and myeloid leukemia via DNA-protein crosslinks at exposures >2 ppm; it induces oxidative stress and cytotoxicity in respiratory epithelium.[36] Acetaldehyde (Group 2B) exhibits genotoxicity through DNA adducts, contributing to oesophageal cancer risk. Trichloroethylene (Group 1) causes kidney cancer via glutathione conjugation metabolites.[37] 1,3-Butadiene (IARC Group 1) causes leukemia/lymphoma via epoxide metabolites (EB, DEB), forming DNA-guanine adducts. Styrene (Group 2A) induces oxidative stress and chromosomal aberrations linked to lymphohematopoietic cancers. Vinyl chloride (Group 1), metabolized to chloroethylene oxide, causes hepatic angiosarcoma through DNA alkylation. Xylene isomers exhibit neurotoxicity via solvent-induced CNS depression and ototoxicity.[38,39,40]

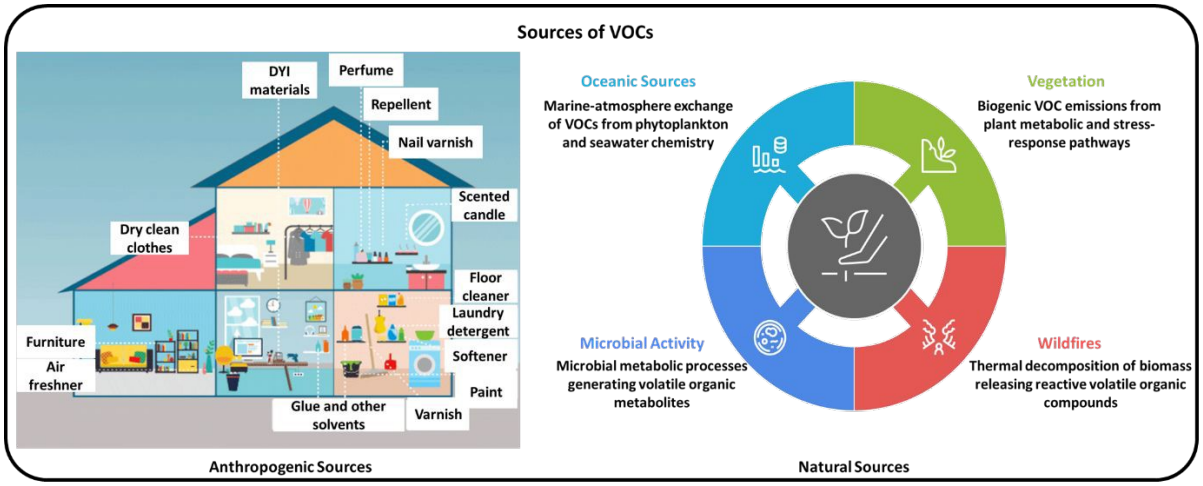

Fig.1 Sources of VOC from indoor and outdoor environments

1.1.3. Environmental Impacts:

VOCs contribute to the formation of tropospheric ozone, photochemical smog, and secondary organic aerosols through NOx photochemistry.[41] Biogenic isoprene (62% global VOC flux) and anthropogenic aromatics dominate secondary organic aerosol (SOA) formation through low-volatility oxidation products, contributing 20-50% to global radiative influence.[42] Wildfires significantly amplify secondary organic aerosol (SOA) yields by 2-5 times via furan chemistry, where furans (highly reactive heterocyclic VOCs emitted during biomass burning) undergo nighttime oxidation, producing secondary brown carbon and contributing to aerosol mass and optical properties. Oxidation of formaldehyde to formic acid is also a key acid-rain precursor pathway, aggravating environmental

View Article Online
DOI: 10.1039/D6NA00239K

acidification from VOC emissions.[43,26] This multi-phase VOC chemistry feedback intensifies regional climate impacts.

These diverse health and environmental impacts necessitate continuous, selective VOC detection across multiple scales, from ppb-level breath biomarkers to industrial compliance monitoring which can be addressed through advanced sensor applications, as discussed in the next section.

1.1.4. Applications of VOC Detection

VOC detection refers to the process of detecting low concentrations of gases, specifically VOCs emitted during industrial, human, and environmental activities by various sensing devices, such as metal oxide semiconductors, electronic noses, and miniature gas chromatography devices. Fig. 2, shows key application areas of VOC detection which includes but not limited to Indoor air quality monitoring, medical diagnostics, environmental monitoring, food quality assessment and Pollution control.

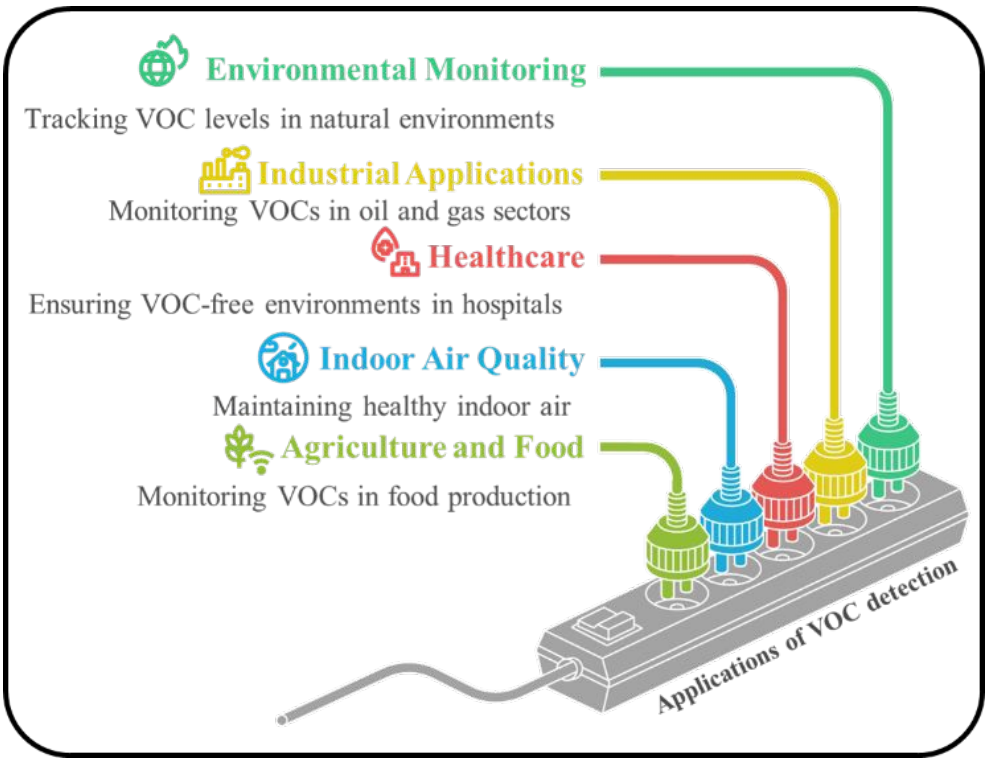

Fig.2 Overview of key applications of VOC detection

- **Environmental Monitoring**: The use of VOC detection instruments has applications in urban air quality measurement, soil contamination detection, roadside emissions tracking, and industrial perimeter surveying, among other activities, in identifying

View Article Online
DOI: 10.1039/D6NA00239K

pollution trends and ensuring regulatory compliance.[44] Mobile and fixed sensors enable precise mapping of VOC sources in cities, facilitating targeted interventions as demonstrated in wastewater and ambient air studies.[45] Nanostructured metal oxide sensors provide sensitive detection of hazardous VOCs from industrial emissions and roadside traffic, aiding in hotspot delineation and environmental protection.[46]

- **Industrial applications including Oil & Gas sectors**: VOC detection in industrial and oil & gas sectors supports emissions control in petrochemicals, manufacturing, waste treatment, and refineries through leak detection, worker safety enhancement, and emission reduction.[47] Advanced sensors enable real-time monitoring of VOC leaks in harsh environments, ensuring compliance and preventing hazardous exposures, as outlined in studies on wireless wearable devices. These technologies facilitate precise source identification in refineries and petrochemical plants, minimizing environmental impact and operational risks
- **Healthcare:** VOC detectors play a major role in the analysis of human breath , and therefore an emerging technology in identifying disease biomarkers for cancer, diabetes, and respiratory diseases, owing to its non-invasive nature of diagnostics.[48] Sensor technology can be integrated onto a wearable device, which are currently being developed, will allow real-time monitoring of their health , thus allowing early detection of diseases while providing alternatives to traditional diagnostic methods.
- **Indoor Air Quality**: VOC sensors can detect the quality of indoor air, particularly in office and work environments, buildings, as well as homes. Detecting VOCs emitted from cleaning agents, paints, and building materials, thus offers mitigating the health risks and establishes the need for suitable ventilation.[49] The ability to offer real-time monitoring for ventilation purposes, as discussed in various studies on monitoring devices in educational and residential establishments, has ensured compliance with healthy building standards, reducing exposure to harmful volatile compounds.[50] Portable and integrated devices help to comply with standards of healthy buildings, which eliminate exposure to damaging volatile compounds. [51]
- **Agriculture and Food**: The detection of plant emitted VOCs such as terpenes in agriculture using VOC sensors helps in the early detection of the onset of stress caused by pathogens, drought, or pests before they develop visually, similar to the usage of commercial indoor air quality sensors that focus on detecting these traces in the air. Similarly, in food, intelligent gas sensors such as MOS-based sensors focus on the

View Article Online
DOI: 10.1039/D6NA00239K

detection of microbial volatile organic compounds (MVOCs), particularly for detecting spoilage in meat products, sea products, and even dairy products, thereby performing real-time assurance for the quality and safety of these products. Similarly, the employment of smart MVOC detection technologies with the aid of GC-MS helps in the detection of spoilage in various food products.[52,53,54] The areas identified in the above-said applications, i.e., medical diagnostics and food safety, have a tremendous potential for employing the usage of VOC sensors, and the same has been explained further in the below sections in the form of case studies for specific products in these fields.

1.1.4.1. Medical diagnostics

VOCs are disease biomarkers specifically in the technique of breath analysis, which is done non-invasively. It has been shown that patients with type-1 diabetes have acetone levels above 1800 ppb, whereas increased levels of ethanol and ethylbenzene are specific markers for fatty liver and lung cancer, respectively.[55] N-propanol is also a key lung cancer biomarker (with major risks factors including pollution, tobacco, and alcohol) with concentrations of 150 ppb in healthy vs. an approximate concentration of 500 ppb in patients.[56]

Liu et al. developed a SnO_2-ZnO composite sensor from ZIF-8-derived ZnO, which features a porous morphology (confirmed by FESEM) that enhances active site exposure and prevents agglomeration.[56] The 5% SnO_2-ZnO showed increased surface area (17.413 m^2/g vs. 11.223 m^2/g for pure ZnO), reduced band gap (3.15 eV vs. 3.20 eV), and higher adsorbed/defect oxygen (6.24%/40.82%), achieving 0.05 ppm LOD for n-propanol with 3/8 s response/recovery times. When the sensor was tested on simulated cancer breath (500 ppb) and five healthy samples, it showed distinguished responses (~3 vs. ~12) across 50-90% RH; however, its only drawback is its high operating temperature (200 °C).

1.1.4.2. Food Safety and Quality Control

Food contamination causes ~600 million illnesses and 0.42 million deaths annually (WHO), with microbial spoilage producing characteristic VOCs as metabolic fingerprints.[1957] Pathogens such as Salmonella (ethanol, acetic acid, hexanal), E. coli, and Aspergillus flavus (hexanal, benzaldehyde for aflatoxins) emit distinct VOC profiles, which are linked to high mortality rates (Salmonella: 31%, Listeria: 28%, E. coli: 3%). Meat rancidity releases 3-methyl-1-butanol and hexanol, whereas fruits exhibit shifts in

VOCs during ripening (77-93% esters, 5-16% alcohols) and spoilage markers like ethyl hexanoate in apples.[19,57]

Okechukwu et al. developed room-temperature GO-SnO_2 nanorods for the detection of aflatoxin-related VOCs, synthesized via chemical methods. Despite reduced surface area (16.4 m²/g vs. 44.3/54 m²/g for pure GO/SnO_2), reactive oxygen O(α) increased (54% vs. 38%), yielding hexanal sensitivity of 0.17, response/recovery times of 145/99 s, and LODs of 0.3 ppm (hexanal), 0.4 ppm (benzaldehyde) and 1.9 ppm (octanal). Pure components showed poor/no response, highlighting composite synergy for food spoilage monitoring.[58]

While VOC detection technologies show remarkable promise across various critical domains, traditional methods face substantial limitations that hinder widespread adoption. The following section examines these challenges and the need for next-generation sensing solutions.

1.1.5. Limitations of traditional VOC detection methods

Traditionally established VOC detection methods include mass-based sensors, electrochemical sensors, electrical sensors (e.g., field-effect transistors, or FETs), optical sensing methods, gas chromatography-mass spectrometry (GC-MS), and photoionization detectors (PIDs). GC-MS analysis requires 15-60 minutes per sample, with high costs per sample. PIDs on the other hand, although provide portability by enabling UV ionization of low-energy VOCs, they suffer from poor selectivity because they cannot discriminate between compounds with similar ionization potentials.[59] cross-react with interferents such as water vapor and aromatics, reducing accuracy by 20-50%.[60,4] GC-MS offers high accuracy but requires expensive equipment, skilled operators, high power consumption, and extended analysis times, which limit its field deployment.[4] Electrochemical sensors offer low power but suffer from drift and poisoning, while optical methods, such as Nondispersive Infrared sensors (NDIR), provide high specificity; however, they are limited to specific VOCs and exhibit poor ppb sensitivity.[10,61]

Table 2. Comparative Overview of VOC Sensor Technologies: Principles, Limitations, and Performance Enhancements

Sensor type	Principle	Limitations	Improvements
Gas-Chromatogram-Mass Spectrometry (GC-MS)	GC separates VOCs based on their boiling points and interactions in a capillary column, producing a time-based chromatogram. Mass spectrometry (MS) then ionizes the separated VOCs, fragments them, and analyzes mass-to-charge ratios to generate unique spectral fingerprints for precise identification and quantification at ppb levels.	Costly, bulky, power-intensive operation, reliance on skilled personnel for interpretation, not portable	Miniaturization-Developing portable GC-MS systems using micro-electromechanical systems (MEMS) and lab-on-a-chip technologies to reduce size/power. Automation-Integrating AI-driven software for real-time data analysis, reducing human error and expertise dependency.
Photoionization Detectors (PIDs)	It is made up of two polarized electrodes, and when VOCs are introduced, photon-induced ionization takes place, causing ions to move toward the electrodes and produce a change in current.	Inability to distinguish gases with overlapping ionization energies (eg., benzene vs toluene)	Hybrid systems- Pairing PID with pre-concentration techniques (eg., adsorbent tubes) or supplemental sensors (eg., metal-oxide semiconductors) to enhance selectivity. Advanced algorithms- Use of machine learning to deconvolute mixed signals by analyzing ionization patterns and temporal response curves.
Electrochemical/ Electrical Sensors	Mainly consists of counter electrode and working electrode. The electrodes are immersed in an electrolyte solution where the gases diffuse through a porous membrane to an electrode where it is either oxidized or reduced and produce an electrical response. Electrical sensors on the other hand are based on interactions between VOCs and sensor resulting in a change in resistance/ current.	Cross-sensitivity to humidity/temperature and short lifespans due to electrode integration	Self-calibration-Incorporating of temperature/humidity sensors for real-time signal correction.

View Article Online
DOI: 10.1039/D6NA00239K

Optical sensors	Consists of a light emitting element, a photo-detecting element, gas sensing element. Based on the principle of interaction of light with a material which can either absorb or transmit the light.	Limited portability and high costs for high-resolution systems	Plasmonic sensors-use gold/silver nanoparticle arrays for surface-enhanced Raman spectroscopy (SERS), enabling ppb-level detection. Low-cost spectroscopy-Leveraging smartphone-integrated spectrometers with cloud-based analysis for field use.
Field-Effect Transistors (FET) sensors	It primarily includes the drain and source electrodes with charge carriers in between, and when VOC interacts with it, the electrical properties such as mobility and threshold voltage are altered.	Expensive, Poor reproducibility and baseline drift	Array configuration-Deploy sensor arrays with varied functionalization to mitigate false positives.

Table 2 indicates the merits and demerits of conventional gas sensing methods, focusing on the essential issues of the working principles, limitations, and proposed improvements. From the inherent limitations of the conventional methods, including their cost, poor portability, cross-sensitivity, and low response, the need arises to utilize the benefits of nanomaterial-based gas detectors, as discussed below.

2. Rationale for SMO heterojunctions and light activation

As already mentioned, conventional gas sensors, including amperometric, catalytic, and semiconductor metal oxide gas sensors, generally require high operating temperatures ranging from 150 °C to 500 °C. This allows maximum ionic conductance, catalyst activity for gas reactions, and adsorption of oxygen on the sensor surfaces. Moreover, at high temperatures, the number of electron-hole pairs increases in semiconductor sensors, while at low temperatures, the chemical reactivity of the gas sensors reduces because of the reduced adsorption of oxygen on the device surfaces. However, the chief disadvantages of these semiconductor metal oxide-based sensors are the incorporation of heaters, which eventually add up to their cost and device complexity in addition to potential ignition of several combustible gases in high-temperature environments.[62,63,64] Additionally, the thermal effects

View Article Online
DOI: 10.1039/D6NA00239K

result in the ripening of the nanoparticle surfaces of the gas sensors, moreover destroying the electrical devices of the detecting system.

2.1. Light-activated room temperature gas sensors: A promising approach towards the next generation of sensor technology

There is a growing interest in overcoming the aforesaid challenges experienced by the conventional sensors by devising efficient gas sensors that perform effectively at room temperature. One of the promising techniques adopted to achieve better efficiency is light activation. This process creates photo-induced electron-hole pairs when the semiconductor is exposed to light of specific wavelengths corresponding to the bandgap of the semiconducting material. This provides the sensor better efficiency compared to other conventional sensors. However, a major drawback of using pure semiconducting sensors is the recombination of electron-hole pairs, which adversely affects the efficiency of the sensor. This problem is efficiently overcome by designing heterojunctions, which are the interfaces between the surfaces of two semiconducting materials. This ensures the separation of the heterojunction because of the alignment of the Fermi level.[65,66] This also ensures the broadening of the light absorbed by the sensor to accommodate a variety of applications.[67,68]

The types of heterojunctions are schematically shown in Fig.3 and are explained below:[69]

- **Type-I (Straddling gap):** In this case, the conduction and valence bands of Semiconductor B are completely within the bandgap of Semiconductor A, resulting in the accumulation of photogenerated electrons and holes in one semiconductor. This results in low redox activity of the semiconductor due to inefficient charge separation and high rates of charge recombination.
- **Type-II (Staggered gap):** The conduction and valence bands are staggered, resulting in the spatial separation of electrons and holes between the two semiconductors (i.e., electrons in Semiconductor A and holes in Semiconductor B), thus improving charge separation.
- **Type-III (Broken gap):** The band gaps of the two semiconductors A and B do not overlap, thus impeding the separation of charge carriers and thereby reducing the photocatalytic activities.
- **S-Scheme Heterojunction:** This junction consists of two semiconductors, A and B, that are staggered. However, unlike the Type-II junction, in this junction, the high-energy electrons from the reduction photocatalyst and the high-energy holes from the oxidation

View Article Online
DOI: 10.1039/D6NA00239K

photocatalyst are retained selectively. This process increases the redox potential by the recombination of the low-energy electrons at the interface.

- **Laddered Type-I Heterojunction:** Here, in this junction, there is a step-like alignment of the conduction band and valence band of one semiconductor with respect to the other. Band alignment of this type is particularly helpful in directing carrier migration and accumulation in devices with band gap values lower than those of the employed semiconductor, improving charge confinement and enhancing photogenerated carrier utilization.[65]
- **Z-scheme:** This behaviour is analogous to a Type-II heterojunction with staggered band gaps, where the Fermi level of Semiconductor B lies higher than that of Semiconductor A, allowing electrons to move in the same direction upon contact. This reinforces gas sensing performance due to the synergetic effects of the two semiconductors and an extended range of light absorption by boosting charge separation through heterostructures.

The type of light source applied, mostly UV or visible LEDs, relies significantly on the bandgap energies of the semiconductors and the target sensing application. Light-activated sensors can be run at much lower power and may enjoy better stability by avoiding high operating temperatures. Yet there are real challenges to overcome, such as uniform illumination, fitting compact light sources into devices, and retaining overall robustness. The increasing need for efficient room-temperature gas sensors has brought to light the shortcomings of conventional high-temperature methods and the potential of light-activated gas sensors. For the ease of readers, we classify the sensor operating temperature regions as: (i) room-temperature (RT) sensing, where the ambient temperature does not exceed 30 °C and there is no external heating; (ii) low-temperature (LT) sensing, where the operation happens in the range 30 °C – 100 °C; and (iii) high-temperature (HT) sensing, where the operation is above 100 °C.

By imbibing the concept of heterojunction engineering, it is possible to design gas sensors with improved charge separation and spectral response capabilities, thereby overcoming some of the most important challenges in the field of gas sensors, including power consumption and sensitivity. These developments pave the way for the investigation of particular gas sensor designs that leverage these. [70,71]

Having outlined the motivation and mechanisms for enhancing gas sensor performance via light activation and heterostructures, the next sub-section delves into the underlying principles of chemiresistive semiconductor metal oxide (SMO) gas sensors. It is crucial to

View Article Online
DOI: 10.1039/D6NA00239K

have a clear understanding of the sensing mechanism, material properties, and important operating parameters before venturing into more sophisticated heterojunction-based structures.

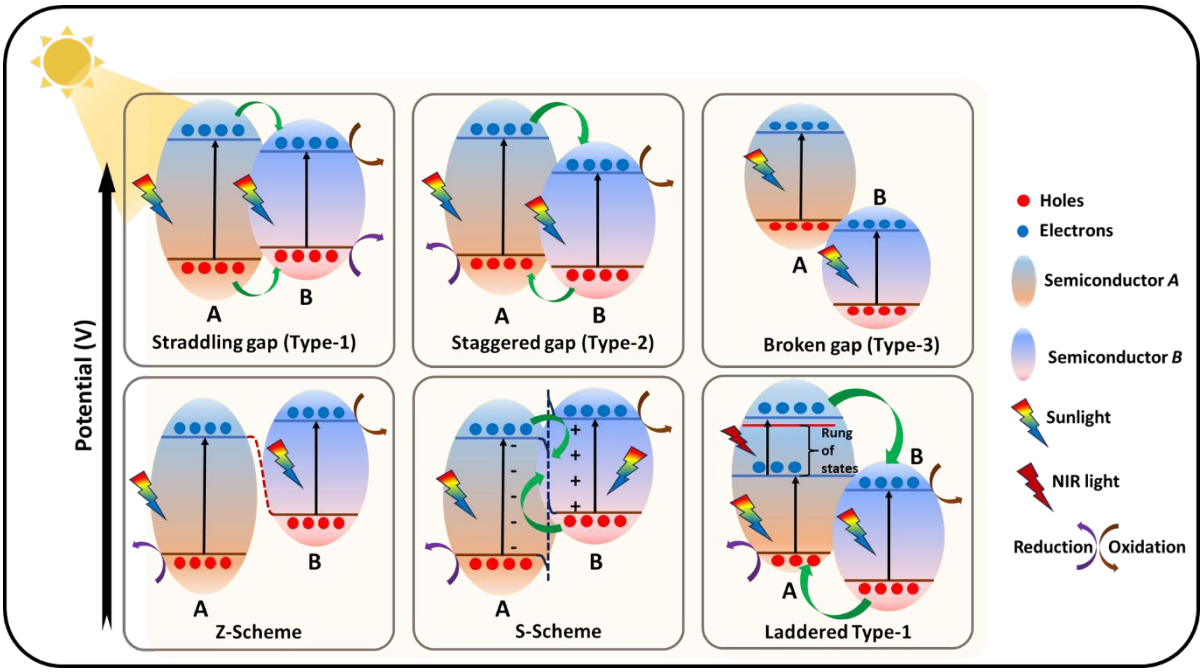

Fig.3 Classification of heterojunction based on band alignment and charge carrier transfer

2.2. Chemiresistive Semiconductor Metal Oxide (SMO) Sensors: Fundamentals

Semiconducting metal oxides with sizes ranging from 1 to 100 nm have attracted significant attention in gas sensing applications due to their exceptionally high surface-to-volume ratio, enhancing the number of active sites for gas adsorption.[72] The first application of semiconducting metal oxides in chemiresistive gas sensors was reported in 1952 by Brattain and Bardeen, who first showed the potential of these materials.[73,74] Later, in 1962, T. Seiyama made further progress in this area by using semiconductor metal oxides to detect gases like toluene, benzene, carbon dioxide (CO_2), propane, and ether at relatively high temperatures of about 400 °C.[74] Chemiresistive gas sensors have several advantages, including ease of operation, low cost, and compatibility with existing electronic circuits.[75] These gas sensors can be broadly classified into two types depending on the type of charge carriers, namely n-type sensors in which electrons are the majority charge carriers, and p-type sensors in which holes are the majority charge carriers. Their ease of fabrication, availability of versatile and sensitive materials, and ease of signal interpretation have made them successful in commercial applications.[76] The working principle of chemiresistive gas sensors relies on the measurement of changes in electrical resistance caused by the interaction of target gases with the sensor surface, as shown in Fig. 4. This interaction primarily involves surface-adsorbed oxygen

View Article Online
DOI: 10.1039/D6NA00239K

species reacting with incoming gases, which can be either oxidizing (e.g., NO_2, O_3, Cl_2, CO) or reducing (e.g., NH_3, CO, HCHO, H_2, H_2S, and other VOCs) in nature.

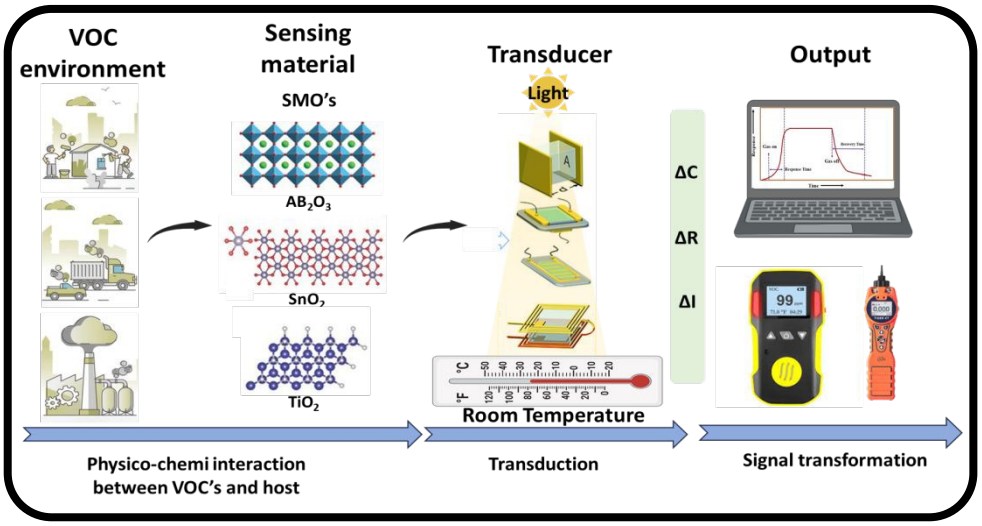

Fig.4 Schematic representation of the VOC sensing mechanism

For n-type semiconductors, exposure to oxidizing gases generally leads to an increase in resistance, while reducing gases cause resistance to decrease; the opposite behaviour is observed for p-type semiconductors.[71] These adsorbed oxygen species extract electrons from the sensor material, creating an electron depletion layer in n-type sensors or a hole accumulation layer in p-type sensors, which underpins the resistance changes.[71] The response to oxidizing and reducing analytes under dark conditions and light illumination conditions is shown in Fig. 5. The response in the presence of both analytes is found to be enhanced under light illumination.

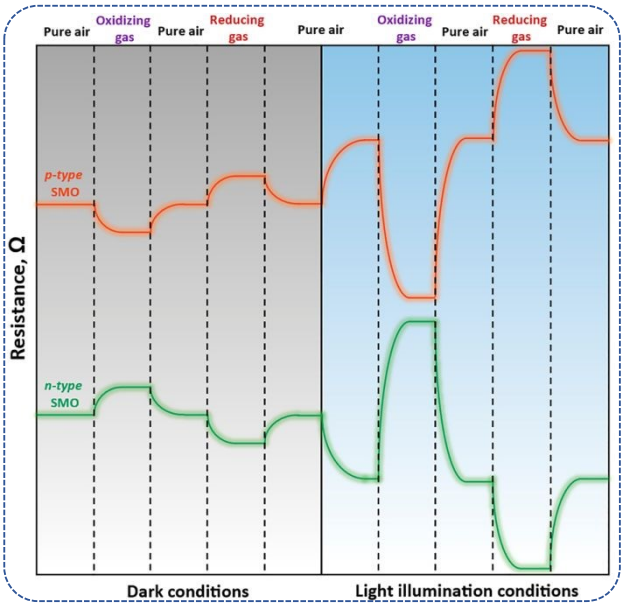

View Article Online
DOI: 10.1039/D6NA00239K

Fig.5 Illustration of SMO gas-sensing responses to oxidizing and reducing gases in the dark and under light exposure. Reprinted from Frontiers in Chemistry, Vol 13, Nasriddinov A, Zairov R, Rumyantseva M, Light-activated semiconductor gas sensors: pathways to improve sensitivity and reduce energy consumption, Copyrights (2025) with permission from Frontiers.[17]

2.3. Oxygen adsorption/desorption mechanisms

The adsorbed oxygen species on the SMO surface initially undergo physisorption, where oxygen molecules (O_2) physically adsorb onto the material. Due to oxygen's high electron affinity, electron transfer occurs from the sensor surface to these molecules, converting them into chemisorbed species.[77,78,79]

$$\frac{1}{2}O_2 + sensor_{\,surface} \leftrightarrow O_{ad-surface} \quad \text{(physisorption)} \qquad (1)$$

The dominant oxygen species vary with operating temperature: below 150 °C, the ionized molecular form O_2^- predominates, while above 150 °C, atomic species such as O^- and O^{2-} become dominant. These transitions correspond to temperature-dependent reactions as follows:

$$O_2(g) + e^- \leftrightarrow O_2^-(ads) \qquad [80\text{-}150\ ^\circ C] \qquad (2)$$

$$O_2(g) + 2e^- \leftrightarrow 2O^-(ads) \qquad [150\text{-}260\ ^\circ C] \qquad (3)$$

$$O_2(g) + 4e^- \leftrightarrow 2O^{2-}(ads) \qquad [>300\ ^\circ C] \qquad (4)$$

Under the illumination of light, the adsorption-desorption equilibrium of oxygen is affected by the presence of photogenerated charge carriers. The photoexcited electrons are caught by the adsorbed O_2, leading to the creation of reactive superoxide oxygen ions, whereas photogenerated holes help in the desorption of oxygen species by neutralization of surface ions. This process increases surface reactivity and speeds up the redox reactions with VOCs, resulting in improved sensor response and faster recovery times. It also maintains steady performance due to the continuous supply of active photogenerated oxygen at room temperature.

These photo-modulated chemisorbed oxygen species then react with reducing target gases, acting as active sites on the surface. The presence of reducing gases leads to the interaction of adsorbed oxygen species with VOCs, which results in their oxidation and the release of electrons again into the sensing material, as given in (eq-5).

$$R(Reducing\ gas) + O^-(ads) \rightarrow RO + e^- \qquad (5)$$

View Article Online
DOI: 10.1039/D6NA00239K

This electron reinjection reduces the depletion layer thickness in n-type sensors (decreasing resistance) or modulates hole accumulation in p-type sensors, producing a measurable resistance change. Thus, the combined light-driven energy, faster oxygen kinetics, and heterojunction-induced charge separation maximize the modulation in the electrical properties. As a result, this leads to improved sensitivity, accelerated response kinetics, and enhanced overall performance of the sensor.

2.4. Pristine SMO Sensors: Response to Reducing/Oxidizing Gases

Based on the basic sensing mechanisms related to oxygen adsorption and charge transfer discussed in the previous section, pristine semiconductor metal oxide (SMO) sensors utilize these phenomena to sense gases based on changes in electrical resistance.

In pristine SMO sensors, electrons are the majority carriers, and holes are the minority carriers. When oxygen molecules adsorb on the surface of the sensor, they capture electrons from the conduction band, forming an electron depletion layer (EDL) in n-type materials or a hole accumulation layer (HAL) in p-type materials. These layers work as barriers to charge transport in the sensor.

For instance, in an n-type semiconductor like SnO_2, upon exposure to reducing gases such as carbon monoxide (CO), a reaction occurs between the gas molecules and the surface oxygen species, resulting in the release of electrons into the material. This causes a reduction in the width of the EDL and a corresponding decrease in the sensor resistance. On the other hand, exposure to oxidizing gases such as nitrogen dioxide (NO_2) results in the reduction of additional electrons, increasing the EDL and the sensor resistance.

In p-type materials like NiO, the sensor resistance increases in response to reducing gases and decreases in response to oxidizing gases due to variations in the HAL. These sensor resistance variations are predictable and useful for selective and sensitive gas detection, which is crucial in applications spanning environmental sensing to industrial safety. Despite their benefits of simplicity and high sensitivity, pristine SMO sensors also have limitations such as low selectivity, drift in the baseline, and instability at high temperatures. These drawbacks trigger the need for the development of sophisticated sensing platforms such as heterojunctions and light-activated sensors, which have been discussed in the previous sections.

View Article Online
DOI: 10.1039/D6NA00239K

2.5. Key Performance Metrics

To assess the effectiveness of chemiresistive SMO gas sensors, there is a need for standardized quantitative parameters that can measure their performance. The performance parameters, known as key performance indicators (KPIs), include response, limit of detection (LOD), selectivity, response and recovery time, and stability as stated in Table 3.

- **Sensitivity**

This is the magnitude of the sensor's response to gas concentration changes, measured by the slope of the calibration curve (resistance vs. concentration). The greater the slope, the greater the sensitivity.

For **n-type sensors** (reducing gases):

$$S = \frac{R_a}{R_g} \quad (6)$$

For **p-type sensors** (reducing gases) or **n-type** (oxidizing gases):

$$S = \frac{R_g}{R_a} \quad (7)$$

Percentage sensitivity: $\left(\frac{R_a - R_g}{R_a}\right) \times 100\%$ (8)

- **Limit of Detection (LOD)**

LOD is the lowest concentration of the analyte that gives a signal distinguishable from noise, calculated as LOD = 3σ/S, where σ is the standard deviation of the noise in the baseline, and S is the sensitivity slope. Sub-ppm LOD values are required in VOC analysis; they indicate the lower detection limit, not the highest.

- **Selectivity**

Selectivity is a measure of the sensor's preference for detecting target gases in the presence of interferents, expressed as selectivity coefficients response patterns in arrays. Untreated SMOs have low selectivity because of their similar VOC adsorption energies.

- **Response and Recovery Time**

Response time (t_{res}): Duration at which the measuring resistance reaches 90% of final resistance change upon gas exposure.

Recovery time (t_{rec}): Duration at which the measuring resistance return to 90% baseline after gas removal.

View Article Online
DOI: 10.1039/D6NA00239K

Fast kinetics (<30 s) are essential for real-time applications; slow recovery times indicate irreversible adsorption.

- **Stability and Reproducibility**

Stability evaluates the stable performance (cycles, storage, or exposure) of the sensor usually requiring <5% drift in 30 days or 100 cycles. Parameters: sintering, poisoning, and humidity. These performance parameters serve as crucial benchmarks for the assessment of chemiresistive SMO gas sensors and help in the identification of the existing gaps in the pristine architecture. Although pristine SMOs show acceptable sensitivity and response times, their suboptimal LOD, lack of selectivity towards interferents, and poor long-term stability, especially at higher temperatures, limit their applicability to real-world settings. These existing drawbacks point towards the need for innovative approaches that can facilitate room-temperature operation with improved performance, which will be addressed in the following sections.

3. Metal Oxide Heterojunction: Design and Sensing Mechanism

Based on the requirement to overcome the drawbacks of pure SMO sensors, especially the low gas response at room temperature owing to the scarcity of thermal electrons and oxygen species, recent studies have explored metal oxide heterojunctions as a promising strategy. Heterojunction composites can improve the charge separation efficiency and extend the lifetime of photoexcited electrons, making them more accessible for gas-surface interactions. The heterojunctions can improve gas sensing by two main methods: chemical sensitization, which facilitates the target gas adsorption, and electronic sensitization, which modulates the sensor resistance in response to gas exposure.[75] In particular, p-n heterojunctions consisting of heterostructures between various metal oxides have shown remarkable enhancements in gas sensing performance. When two semiconductors with different Fermi levels are brought into contact, electrons will transfer from the material with a higher potential to the material with a lower potential until a balance is achieved. Consequently, a region with a depleted concentration of charge carriers, or depletion region, forms near the interface, along with band bending and the appearance of a potential energy barrier. The electrons must overcome this barrier to cross the interface, thus modulating the charge transport and gas sensing performance.

The combined effect of metal oxide heterojunctions can increase the number of active sites for gas adsorption, increase the concentration of oxygen vacancies, and modify the band

View Article Online
DOI: 10.1039/D5NA00239K

structure, which can result in enhanced sensitivity and selectivity. This strategy can effectively overcome the challenges discussed in the previous sections, providing a solution for the development of high-performance room-temperature gas sensors.

The synergistic effect in metal oxide heterojunctions enhances the number of active sites for gas adsorption, the concentration of oxygen vacancies, and the band structure, thus improving sensitivity and selectivity. This method is an effective solution to the challenges discussed in the previous sections, providing a way to achieve high-performance room-temperature gas sensors.[80]

3.1. Types of Heterojunctions

As explained in Section 2.1, heterojunctions can be classified into different types such as Type I, Type II, Type III, Z scheme, S scheme, and laddered Type I. In this section, we will discuss the doped variants of heterojunctions, namely p-n, n-n, and p-p heterojunctions, which provide more routes for modulating charge transfer and sensing properties.

- **p-n type**

Based on the improved sensing mechanisms provided by metal oxide heterojunctions, the p-n heterojunction is particularly prominent as one of the most efficient structures for improving gas sensor performance. A p-n heterojunction is created by the junction of p-type and n-type semiconductors, resulting in band bending and alignment at the junction.[69]

Table 3. Key performance metrics for VOC gas sensors

Metric	**Definition**	**Typical Target Values**
Sensitivity	$S = R_a/R_g$ or R_g/R_a	>10-50 for VOCs [81]
LOD	$3\sigma/m$	<1 ppm (environmental)
Selectivity	$S_{target}/S_{interferent}$	>5:1 preferred [71]
Response/Recovery	Time to 90% change	<30 s [82]
Stability	% drift over time	<5% (30 days) [83]

At the p–n interface, electrons flow from the n-type semiconductor toward the p-type, while holes move in the opposite direction until their Fermi levels equilibrate. This charge transfer forms a depletion region with a built-in potential barrier that modulates electron transport and band structure, ultimately enhancing gas adsorption and sensor resistance modulation. Recent studies illustrate these benefits through diverse heterojunction designs, such as ZnO–CuO nanorods on ITO substrates grown by Subha et al., where nanogaps expanded the interfacial area to detect ethanol down to 50 ppm with a 9 s response, 420 s recovery, and strong selectivity over H_2S and NH_3.[84]

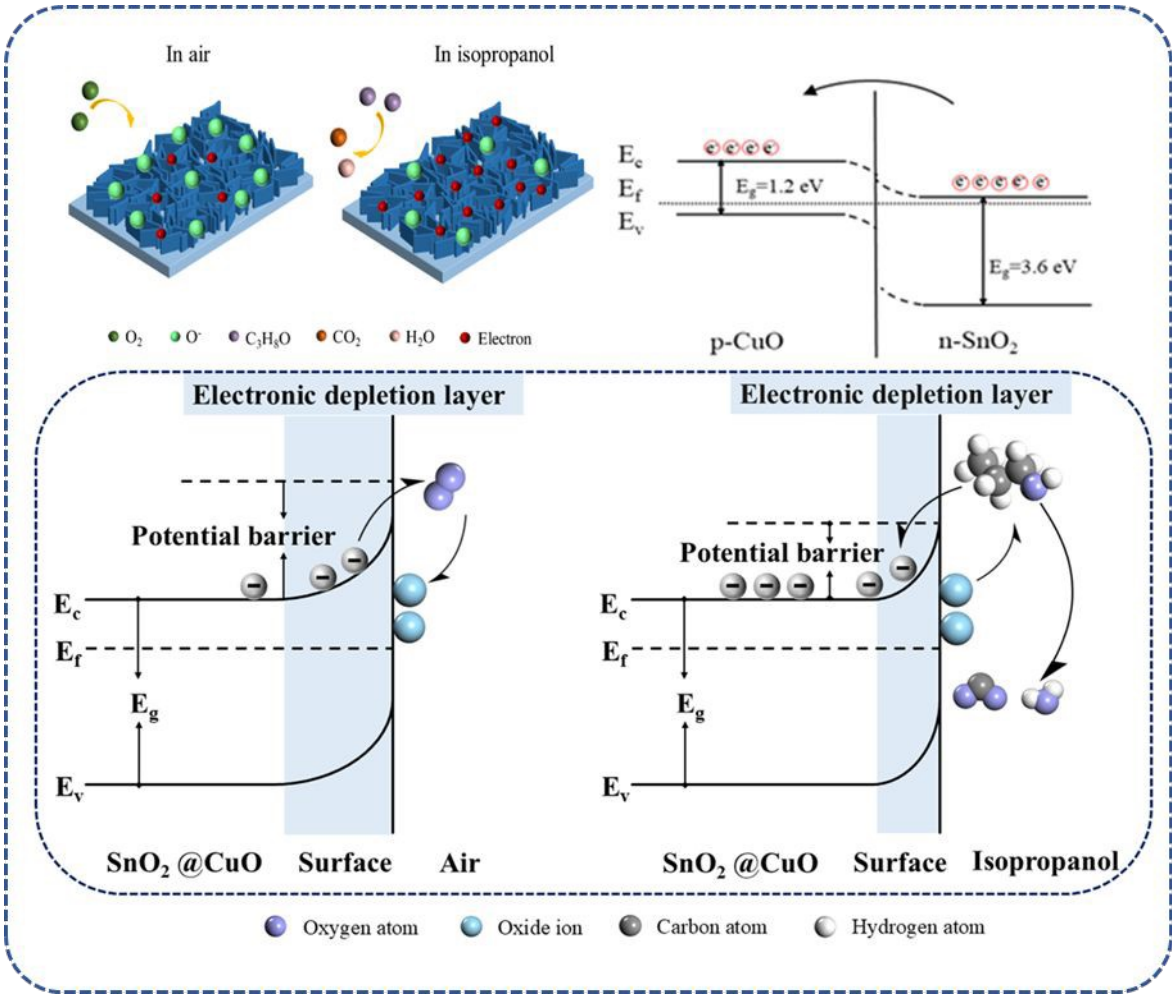

Fig.6 Schematic illustration of the sensing mechanism and energy band structure of porous SnO_2/CuO nanosheets in air and in an isopropanol atmosphere. Reprinted from Materials Research Bulletin, Vol 185, Haibo Ren, Jie Wan, Hui Pan, Jiarui Huang, Facile synthesis of porous SnO_2@CuO nanosheets with highly sensitive performance of VOCs, Copyrights (2025) with permission from Elsevier.[85]

View Article Online
DOI: 10.1039/D6NA00239K

Building on such oxide pairings, Sen et al. employed green synthesis of rGO/Cr^{3+}-doped Fe_2O_3 composites to boost surface area and active sites, yielding a 6.8 response to 10 ppm acetone, a 1 ppm detection limit, 10 s response/recovery times, 150-day stability, and efficacy in breath analysis for diabetes.[86] Similarly, Li et al.'s CuO/In_2O_3 sensor at 70 °C (LT operation) delivered an 8.5-fold response boost over pure In_2O_3 with a 200 ppb H_2S limit,[87] while He et al.'s MXene/SnS_2 heterojunction achieved ammonia detection at 10 ppb, 40/35 s kinetics, and high solvent selectivity. [88] Complementary advances include Chen et al.'s light-illuminated NiO-ZnO for 10 ppb ethanol at room temperature,[89] Ren et al.'s porous SnO_2–CuO microflowers with 51.76 response to isopropanol at 240 °C (HT operation) and 29 ppb limit due to oxygen vacancies (Fig.6),[85] and Jadhav et al.'s SILAR-synthesized Bi_2O_3–TiO_2 with 610% response to 100 ppm $NH3_3$, six-week stability, and humidity tolerance.[90]

- **n-n type:**

Beyond p–n junctions, n–n and p–p heterojunctions offer complementary advantages through distinct band alignments and charge dynamics. Formed between two n-type semiconductors with dissimilar Fermi levels, n–n types enable enhanced carrier separation; for instance, Srinivasan et al. developed a UV-activated ZnO/CdO sensor for acetone disease diagnosis, achieving a 36-fold response boost, 61/47 s kinetics at 1 ppm, and stability down to 1 ppm. [91] Likewise, Liu et al.'s hydrothermally synthesized In_2O_3 microspheres modified with SnO_2 nanorods delivered 66% response to 100 ppm formaldehyde with 21/41 s response/recovery times [92] while Zhao et al.'s sea urchin-like CeO_2–$W_{18}O_{49}$ composite showed 12.2 response to 100 ppm n-butanol at room temperature, which is 4.7 times better than pristine $W_{18}O_{49}$—due to enriched oxygen vacancies and active sites.[93] p–p heterojunctions, such as Kumar et al.'s hydrothermally prepared SnS/$MoSe_2$ nanocomposite, further demonstrate room-temperature ethanol selectivity with 12.32 m²/g surface area, 26.8 response to 400 ppm, 9.1/15.7 s response/recovery times, and 7.6-fold preference over benzene.[94] This heterojunction diversity optimizes VOC sensing across targets and conditions.

- **p-p type:**

Similar to n–n heterojunctions, p–p type heterojunctions also exhibit significant potential for VOC sensing due to their distinct charge transport and surface properties. SnS and $MoSe_2$ are well-known p-type semiconductors, and Kumar et al. utilized their heterojunction to provide outstanding selectivity for ethanol sensing at room temperature. The hydrothermally

View Article Online
DOI: 10.1039/D6NA00239K

synthesized pure SnS and $MoSe_2$ had nanoplate and nanosheet morphologies, respectively. FESEM images of the obtained nanocomposites revealed a perfect combination of these nanosheets and nanoplates.[95] Moreover, BET analysis showed that the nanocomposite's specific surface area increased to 12.32 m²/g, exceeding the 8.23 m²/g of pure SnS. This structural enhancement translated into a superior response value of 26.8 toward 400 ppm ethanol, with faster response and recovery times of 9.1 s and 15.7 s respectively, compared to 12.4 s and 20.3 s for pure SnS. The nanocomposite exhibited pronounced selectivity toward ethanol, with response values 7.6, 3.4, and 2.5 times higher than those observed for benzene, formaldehyde, and acetone, respectively. This outcome highlights the effectiveness of p–p heterojunctions, where tailored morphology and enlarged surface area facilitate enhanced charge transfer and adsorption, thereby markedly improving VOC sensing performance. Such advances complement the well-established benefits of p–n and n–n heterojunction systems, emphasizing the versatility of heterojunction engineering in sensor design. As summarized in Table 4, nanocomposite heterojunctions demonstrate significant advances in VOC sensing at room temperature, with p–p configurations complementing the established benefits of p–n and n–n systems by further improving sensitivity and selectivity.

Table 4 Room-Temperature VOC Sensing Performance of Nanocomposite Materials

Material	**Technique**	**Gases sensed**	**Operating Temperature (°C)**	**Surface area (m²/g)**	**LOD**	**Concentration (ppm)**	**Response**	**Response/ Recovery times (s)**	**References**
Ta_2O_5 @SnO_2/Co_3O_4	Electrospinning-Hydrothermal	Ethanol	25 (RT)	50.5252	522 ppb	500	14.16	98.1/950.4	[96]
SnO_2/rGO	Hummer-	Formaldehyde	27 (RT)	NA	33 ppb (theo	10	9	35/10	[97]

View Article Online
DOI: 10.1039/D6NA00239K

	Hydrothermal				theoretical)				
RGO/TiO_2	Hummer-Hydrothermal	n-butanol	25 (RT)	47.9	2 ppm	85	18	352/506	[98]
rGO/CeO_2	Hummers' method-Microwave assisted hydrothermal	triethylamine	24 (RT)	36.5	1 ppm (theoretical)	100	4.32	78/377	[99]
CuO/Cu_2O	Redox method	n-butanol	22 (RT)	71.6	NA	100	5.9	25/50	[100]
MoO_2/MoO_3/MXene	Hydrothermal	ethanol	25 (RT)	13.54	5 ppm	100	10.8	46/276	[101]
ZnO/CuO	Co-precipitation	n-butanol	# (RT)	NA	4.25 ppm	20	247	19/11	[102]
Pd/PdO/ZnO	Hydrothermal	Formaldehyde	# (RT)	NA	1 ppm	100	38.57	256/264	[103]

TiO_2/ZnO	Solgel-Hydrothermal	2-Propanol	# (RT)	NA	1 ppm	100	68	71/85	104

 # Literatures where the specific room temperature values were not reported

3.2. Band structure and charge transfer mechanism

Having discussed different heterojunction types and their enhanced VOC sensing capabilities, it is essential to explore the underlying band structure and charge transfer mechanisms that govern their improved performance. To get a clearer understanding of the same, the band structure and mechanism of the semiconductor metal oxide heterojunction gas sensor is depicted in Fig.7. As it is known that n-type and p-type semiconductors combine to form heterojunctions, electrons flow from the n-type to the p-type while holes move in the opposite direction until their Fermi levels equilibrate. This process induces upward band bending in the p-type and downward band bending in the n-type, creating a potential barrier that plays a crucial role in sensor function.[80] For example, Ren et al. developed a p–n CuO–SnO_2 isopropanol sensor where UV–Vis analysis revealed a narrowed band gap of 3.06 eV for the composite compared to 3.53 eV for pure SnO_2.[85] This reduction helps in charge transfer as it allows the flow of electrons from the conduction band of SnO_2 to the valence band of CuO and holes in the reverse direction, thus making it less likely for them to recombine. The difference in Fermi levels (5.3 eV for CuO and 4.5 eV for SnO_2) helps in the flow of electrons, thus increasing the space charge region and the potential barrier, hence improving the resistance modulation and sensing properties. Similar charge transfer mechanisms have also been reported by Zhang et al. in UV-activated ZnO-NiO heterostructures, where the electron depletion layer in ZnO and the hole depletion layer in NiO generate an interfacial electric field that increases the sensor response, with NiO acting as a catalyst for the adsorption of oxygen species.[105] In addition, Guo et al. reported the detection of formaldehyde at concentrations as low as 5 ppb using In_2O_3-ANS/rGO composites, where the transfer of electrons from In_2O_3 to ANS/rGO and holes in the reverse direction generates depletion regions and electric fields essential for resistance modulation (Fig.8).[106] These insights unify the structural and electronic bases of enhanced sensing across diverse heterojunction architectures.

Therefore, the importance of band structure and charge transfer processes is emphasized in relation to the role of electric fields and potential barriers at the interface in improving sensor performance. Looking ahead, a new approach that is being explored to further enhance sensitivity and response rates is the use of light activation of semiconductor metal oxide (SMO) heterojunction sensors. This is achieved through the use of photo-generated charge carriers that increase surface reactions and charge transfer processes, offering new possibilities for low-temperature operation and selective VOC detection. The next section delves into recent advances in light-activated SMO heterojunction-based sensors, exploring their unique mechanisms and performance benefits under various illumination conditions.

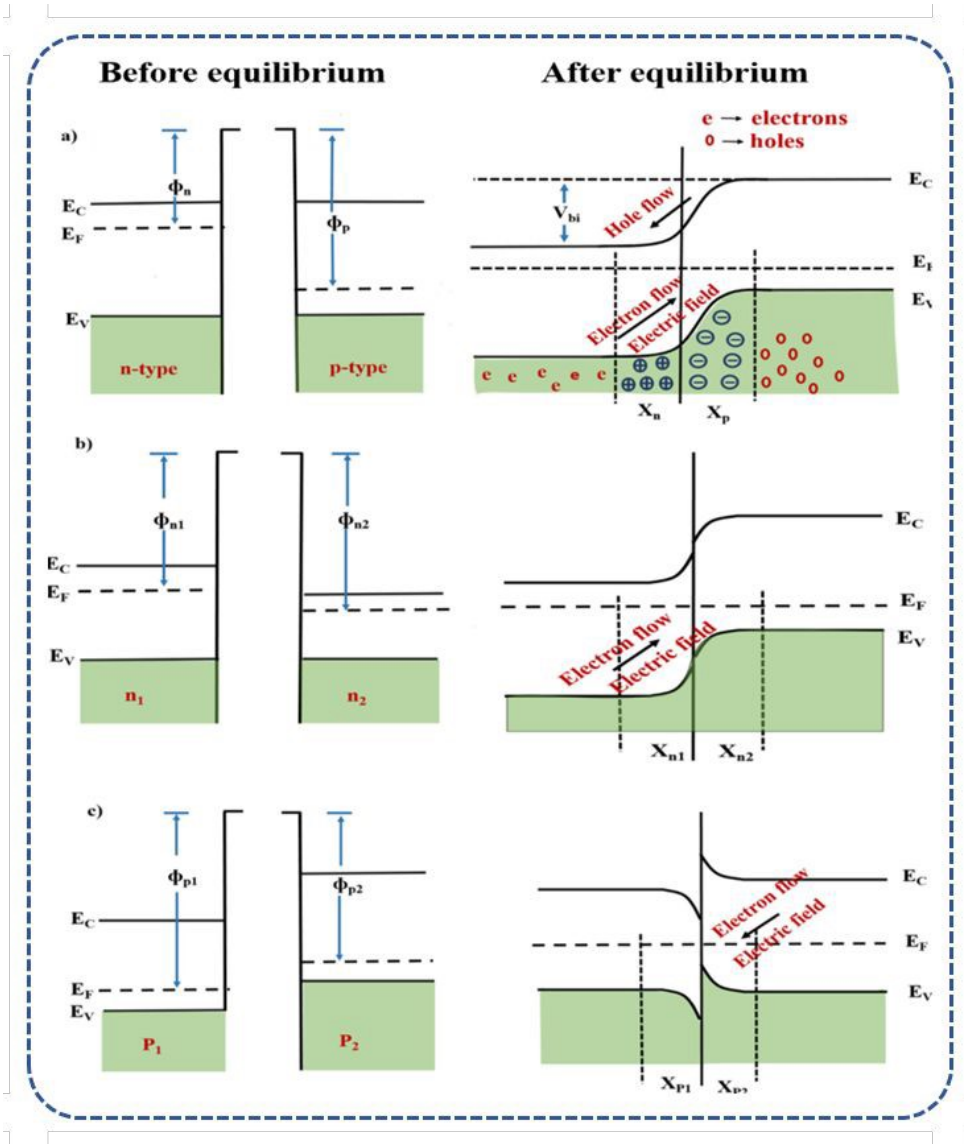

Fig.7 Energy band structure and sensing mechanism of semiconductor metal oxide heterojunction gas sensor. Reprinted from Applied Materials & Interfaces, Vol 15, S. Uma,

View Article Online
DOI: 10.1039/D6NA00239K

M.K. Shobana, Band structure and mechanism of semiconductor metal oxide heterojunction gas sensor, Copyrights (2024) with permission from Elsevier. [80]

3.3. Light-activated SMO heterojunction-based sensors

D.A. Melnick pioneered the concept of light activation for gas sensing.[74] Key considerations for selecting light sources include matching the material's bandgap, which lattice defects can modulate.[64] Under illumination, photoexcitation generates electron-hole pairs that either separate or recombine on the material's surface to drive the redox reactions with analytes, as further supported by recent studies that show superior charge mobility and VOC detection capabilities in state-of-the-art, light-triggered nanostructures, as shown in (eq-9).[107–109]

$$h\nu \rightarrow h^{+}(h\nu) + e^{-}(h\nu) \quad (9)$$

The efficiency of light-activated sensors depends heavily on the photogeneration rate of charge carriers, lifetime, recombination, and interfacial transport along heterojunctions. In unmodified or pristine SMOs, rapid nanosecond recombination of photogenerated electron-hole pairs drastically restricts their availability for surface interactions, suppressing the sensing performance.

Rapid recombination within nanoseconds poses a major challenge by depleting available carriers and impairing the sensor's responsiveness. Despite the difficulty in achieving spatial separation of electrons and holes, heterojunctions have emerged as a viable solution to this issue.

These photogenerated electrons react with adsorbed oxygen (eq-10) while holes recombine with superoxide ions (eq-11), releasing free oxygen and enhancing target gas interactions.

$$e^{-}(h\nu) + O_2 \rightarrow O_2^{-}(h\nu) \quad (10)$$

$$(h^{+}(h\nu) + O_2^{-}(h\nu) \rightarrow O_2) \quad (11)$$

Photo-illumination fundamentally alters the oxygen adsorption-desorption equilibrium by supplying a continuous flow of photogenerated charge carriers. Among these, photoelectrons are caught by the adsorbed oxygen to create highly reactive species ($O_2^{-}, and\ O^{-}$). On the other hand, photogenerated holes neutralize and desorb surface-bound oxygen ions. This continuous process of light-activated oxygen cycling increases the density of active reaction sites and escalates the surface redox kinetics. Thus, the chemisorbed oxygen and VOCs

View Article Online
DOI: 10.1039/D6NA00239K

interact readily under illumination, resulting in enhanced sensitivity, increased reaction rates, and desired lower recovery times. This light-based carrier generation effectively counterbalances the absence of thermally activated charge carriers, enabling these surface reactions to happen at room temperature, avoiding the requirement of high operating temperatures for sensing.

Moreover, visible light offers advantages over UV in terms of cost-effectiveness, low power use, and safety, as UV poses risks to human skin and eyes. Additionally, the detailed analysis of defects, bandgap tuning, and plasmonic enhancements can lead to light absorption in the visible region of the spectrum, in turn boosting the photoactivation efficiency.

In summary, the light-activation-based sensing enhancements stem from the interplay of photogenerated carriers, surface-bound oxygen interactions, and electric fields created due to heterojunction formation. Collectively, these three phenomena cooperatively command the improvement of sensor response, targeted selectivity, and room-temperature operation capability of SMO-based sensors without the need for external thermal activation.

3.4. Light Activation Strategies in Heterojunction Sensors

Based on the underlying principles of band structure and interfacial charge transport, photoactivation has been identified as a highly effective approach for enhancing the performance of semiconductor metal oxide (SMO) heterojunction sensors. Illumination enhances the concentration of charge carriers, improves charge separation at the junction interface, and enhances surface reaction kinetics. The effectiveness of the illumination is strongly dependent on the spectral match between the light energy and the electronic structure of the material. The photogenerated electron-hole pairs result in a greater population of more reactive species at the sensor surface. Here, the heterojunction interface promotes the spatial separation of charge carriers, avoiding their recombination. Because of this, charge carriers show increased participation in oxygen adsorption-desorption processes and enhanced surface reactions with gas, which are crucial for performing sensing under room temperature.

For optimal activation, the energy of the incident photons should be above the bandgap of the semiconductor material while also satisfying its natural absorption characteristics, which are typically modulated by lattice defects, dopant sites, and structural distortions. As a result of increased photon absorption, the rate of electron-hole pair generation is significantly enhanced, resulting in a substantial amplification of the sensor response under illumination.

View Article Online
DOI: 10.1039/D6NA00239K

It is highly important to bring out the clear distinction between ultraviolet (UV) and visible-light activation in SMO-based sensors. UV excitation is usually effective for wide-bandgap semiconductors such as ZnO, SnO_2, and TiO_2. Here, the photon energy matches or exceeds the bandgap, resulting in direct band-to-band excitation leading to the generation of electrons and holes. On the other hand, visible light has a photon energy that is insufficient for bandgap crossing and requires additional bandgap-engineering strategies. These strategies include (a) narrowing of the bandgap via doping or defect engineering, (b) sensitization using carbon-based nanostructures or narrow bandgap semiconductors, (c) constructing heterojunctions, and (d) plasmonic enhancement approach using noble nanomaterials. The mentioned strategies will make sub-band excitation possible and improve the light absorption in the visible spectrum. Additionally, the enhanced charge-separation efficiency will result in active and functional SMO sensors even under low-energy illumination situations.[110–112]

Guo et al. utilized visible light to activate an In_2O_3–functionalized graphene oxide heterojunction sensor detecting formaldehyde at 5 ppb at room temperature.[106] The engineered heterojunction effectively separated photogenerated charges, prolonging their lifetimes and boosting interaction with adsorbed oxygen species, yielding enhanced sensitivity. The sensing mechanism of the sensor under air and upon exposure to formaldehyde under UV light illumination is illustrated in Fig.8.

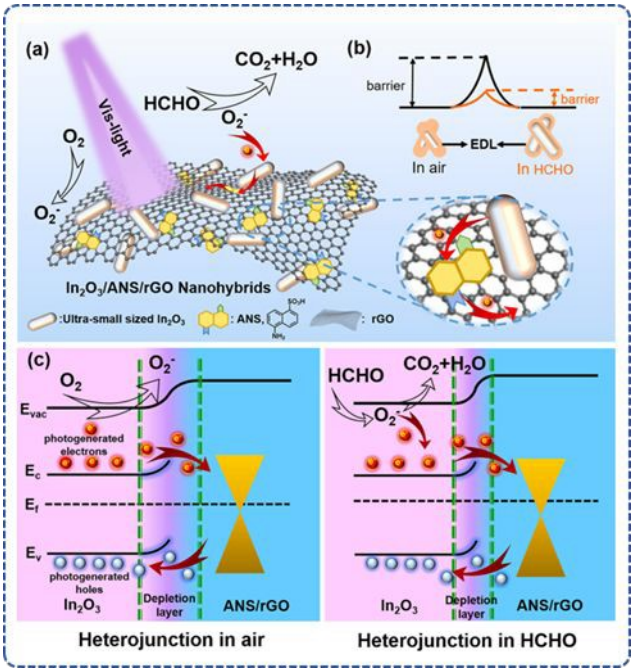

Fig.8 Enhanced sensing mechanism of InAG nanohybrids. (a) Reaction of HCHO molecules on the surface of InAG nanohybrids under 405 nm light illumination. (b) Changes in EDL thickness and potential barrier of In_2O_3 homojunction in air and HCHO. (c) Energy band

View Article Online
DOI: 10.1039/D6NA00239K

diagram of InAG heterojunction in air and HCHO atmosphere. Reprinted from Applied Materials & Interfaces, Vol 15, Lanpeng Guo, Hongping Liang, Huiyun Hu, Shenbin Shi, Chenxu Wang, Sitao Lv, Haihong Yang, Hao Li, Nicolaas Frans de Rooij, Yi-Kuen Lee, Paddy J. French, Yao Wang, Guofu Zhou, Large-Area and Visible-Light-Driven Heterojunctions of In_2O_3/Graphene Built for ppb-Level Formaldehyde Detection at Room Temperature, Copyrights (2023) with permission from ACS

Similarly, He et al. developed a flexible, UV-activated CuO/TiO_2 heterojunction sensor for H_2S detection with significantly improved response metrics and selectivity at room temperature, further showcasing the benefits of heterojunction design in light-activated sensors.[113] Similarly, Zhang et al. demonstrated this concept using a NiO-ZnO heterojunction ethanol sensor prepared via solvothermal synthesis.[105] The incorporation of 3% NiO increased the surface area from 38.99 to 230.54 m^2/g and raised the adsorbed oxygen percentage to 40.65%, enhancing active sites and analyte adsorption (Fig.9). Under dark conditions, the sensor required 330–340 °C for optimal operation, but this temperature dropped dramatically to 65 °C (representing LT operation rather than true RT operation) upon 365 nm UV illumination due to accelerated electron-hole generation and separation at the p–n junction interface (Fig.10). This sensor achieved a low ethanol detection limit of 102 ppb and exhibited a photo-response over 11 times greater than pure ZnO, with high selectivity against common interferents.

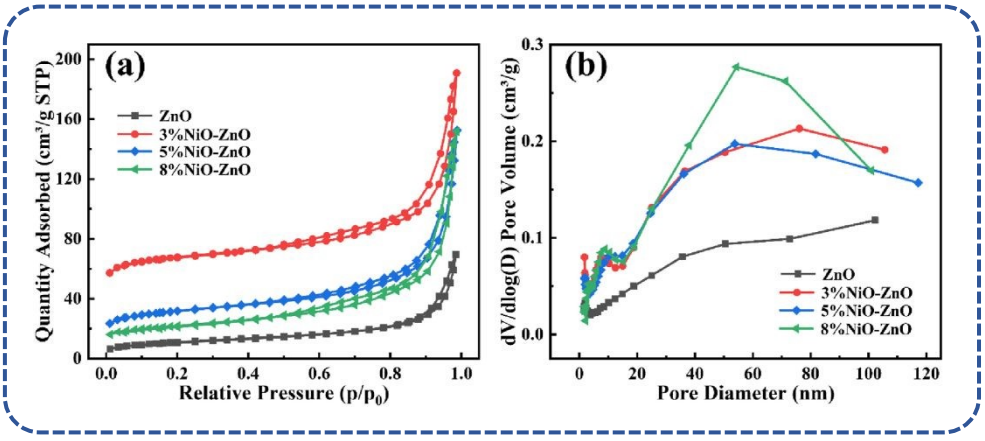

Fig.9 (a) Nitrogen adsorption–desorption isotherms and (b) pore size distribution profiles of ZnO and the NiO–ZnO composite. Reprinted from Materials Science in Semiconductor Processing, Vol 169, Lu Zhang, Yanli Kang, Ying Tang, Feng Yu, UV-Activated ZnO–NiO

heterojunction sensor for ethanol gas detection at low working temperature, Copyrights (2023) with permission from Elsevier. [114]

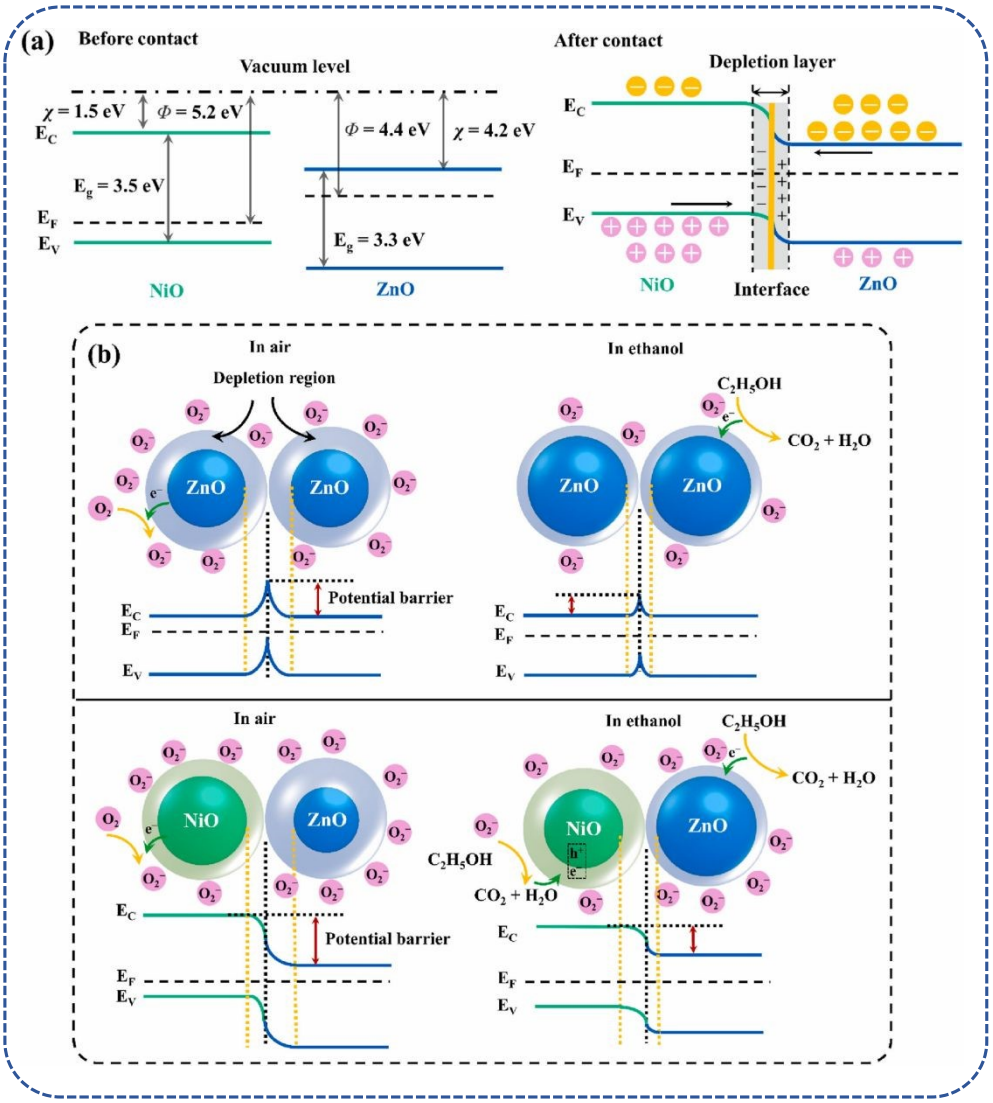

Fig.10 Schematic illustration showing (a) the energy band structures of NiO and ZnO before and after contact, and (b) the sensing mechanisms of pristine ZnO and NiO–ZnO heterostructures. Reprinted from Materials Science in Semiconductor Processing, Vol 169, Lu Zhang, Yanli Kang, Ying Tang, Feng Yu, UV-Activated ZnO–NiO heterojunction sensor for ethanol gas detection at low working temperature, Copyrights (2023) with permission from Elsevier.[114]

Other notable advances include De et al.'s CuO-$CuFe_2O_4$ nanocomposite sensor, achieving high H_2 and ethanol responses at moderate temperatures through redox processes facilitated

View Article Online
DOI: 10.1039/D6NA00239K

by adsorbed oxygen under light activation.[79] Pargoletti et al.[115] combined SnO_2 with graphene oxide under UV light to operate at room temperature, achieving low detection limits and high selectivity for ethanol. Srinivasan et al. reported a UV-enhanced ZnO/CdO n–n heterojunction sensor for acetone with a 36-fold response increase, underscoring the broad applicability of light activation across heterojunction types.[91] Sun et al. synthesized a SnO_2-Y_2O_3 heterojunction nanofiber sensor with absorption extending into the visible range, allowing flexible light source choice. Under UV illumination, it exhibited a 318% performance increase for 10 ppm H_2S with rapid kinetics, corroborated by DFT analysis showing strengthened gas adsorption. [116] Whereas, You et al. engineered a sandwich-structured NiO–Ag–$ZnIn_2S_4$ heterojunction sensor operating efficiently under visible light for triethylamine detection well below occupational exposure limits [117] (Fig.11). The Ag layer enhanced electron transfer and charge separation, highlighting synergistic effects of heterojunctions combined with metal facilitation and light activation.

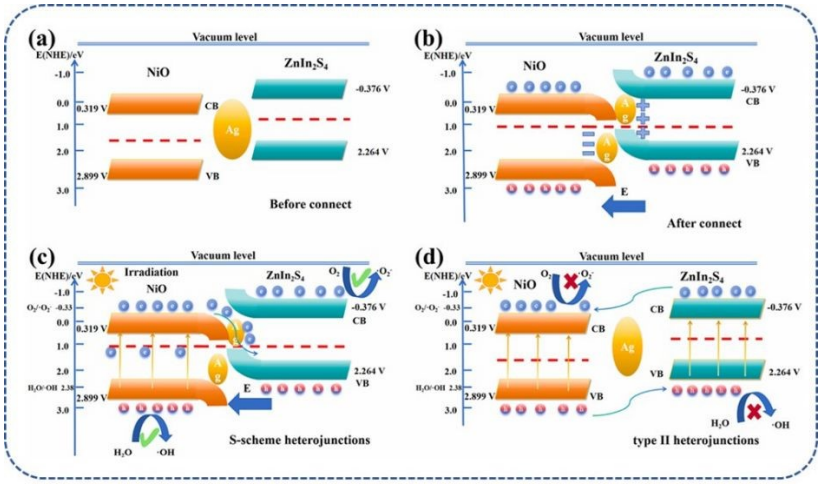

Fig.11 Schematic representation of the energy band alignment of the NiO/Ag/$ZnIn_2S_4$ heterojunction: (a) prior to contact, (b) after contact formation, and (c, d) after contact under light illumination. Reprinted from Talanta, Vol 295, Jianxian You, Yulin Zhu, Dehua Wang, Jiahao Li, Yan Liang, Yanxing Yang, Yong Yang, Enhanced S-scheme mechanism in sandwich-type NiO/Ag/$ZnIn_2S_4$ heterojunction nanoarray for room temperature triethylamine sensing under visible light excitation, Copyrights (2025) with permission from Elsevier. [117]

ZnO/CdO n–n heterojunction sensor for acetone with a 36-fold response increase, underscoring the broad applicability of light activation across heterojunction types.[91] Sun et al. synthesized a SnO_2-Y_2O_3 heterojunction nanofiber sensor with absorption extending into

the visible range, allowing flexible light source choice. Under UV illumination, it exhibited a 318% performance increase for 10 ppm H_2S with rapid kinetics, corroborated by DFT analysis showing strengthened gas adsorption. [116] Whereas, You et al. engineered a sandwich-structured NiO–Ag–$ZnIn_2S_4$ heterojunction sensor operating efficiently under visible light for triethylamine detection well below occupational exposure limits,[117] which is illustrated in Fig.11. The Ag layer promoted electron transfer and charge separation, emphasizing the synergistic effects of heterojunctions and metal assistance and light activation. Taken together, these works, as listed in Table 5, demonstrate the ability to achieve low-temperature, highly selective, and sensitive VOC detection by carefully controlling light wavelength, heterojunction materials, and morphological properties, thus indicating that light-activated SMO heterojunction sensors represent a promising new area in gas sensing. Thus, while UV activation leads to direct and efficient photocarrier generation in wide-bandgap SMOs, visible-light activation, which depends on materials engineering to demonstrate comparable performance, is highly desirable for low-power and practical RT sensing applications.

Another important point worth mentioning here is that the efficiency of light-activated gas sensors is strongly affected by both intrinsic material properties and external illumination conditions. The light source's wavelength, light intensity (or power density), uniformity, illumination geometry, lit area, and separation between the sensor and the light source are important factors. Any variation in these parameters directly affects the generation rate of photocarriers, surface reaction kinetics, and charge-carrier dynamics. Therefore, enhanced sensing performance mentioned in the literature could be due to the improved material design, such as charge separation due to heterojunction formation, or higher illumination intensity, or optimized experimental conditions.[110,118,119,17] Thus, in order to achieve the best reproducibility and allow meaningful comparisons across reports, it is important that these illumination parameters are properly reported as per some reference standard material engineering and carefully controlled illumination conditions during light-activated gas sensing studies.

Although light-activated heterojunction sensors have shown remarkable laboratory results, their successful application in real-world applications requires their smooth integration into practical devices and systems. The following section will discuss approaches to integrate these innovative SMO sensors into wearables, IoT systems, and smart packaging to overcome miniaturization, power, and connectivity issues for continuous VOC detection in various environments.

View Article Online
DOI: 10.1039/D6NA00239K

4. Sensor Integration into devices and systems

Combining light-activated heterojunction sensors within wearable and IoT systems poses bigger challenges in gas sensing, mainly due to the optical excitation requirement. Compared to thermally activated sensors, here, both kinds of optimizations of material properties and illumination parameters need to be performed for practical applications. In a light-activated sensing system, the integration of miniature light sources, viz., UV/Visible LEDs or recently evolved micro-LEDs, is an important consideration. This will help in optimizing the power consumption for prolonged continuous operation, especially in battery-powered wearable devices. Additionally, light-induced heating may create issues of unintended thermal contribution that need to be tackled in such devices. [110,118,]

A notable example is the work by Ghuge et al.[120] demonstrating the development of a TiO_2/MoO_3 triethylamine sensor via spin-coating, achieving 2.35×10^{-3}/ppm sensitivity and 22 ppm detection limit. Integration of UV light source with wireless IoT interfaces, achieves real-time industrial hazard monitoring by combining light-activated sensing with compact electronics as depicted in Fig.13A. Similarly, Li et al.'s hollow Fe_2O_3–NiO heterojunction nanorods (178.3 m^2/g surface area, 0.5 ppb ethanol limit) incorporate voice alerts and GPS tracking for law enforcement applications like drunk driving detection with a schematic animated image as shown in Fig.13B.[121] The device demonstrated the combination of light-activated sensing with IoT connectivity, paving the way for real-time remote monitoring, establishing the applicability of such systems in field-based environments.

In wearable applications, Cheng et al. engineered a flexible, UV-activated TiO_2/YSZ nanofiber sensor for room-temperature exhaled breath analysis. TiO_2 was coated on electrospun YSZ nanofibers via ALD withstood 0.52 MPa tensile stress, delivering 4.8 response to 50 ppm acetone (27.4%/ppm sensitivity) and detecting 1.8 ppm simulated diabetic breath with 1.35 response. Due to their flexibility, these sensors could be embedded in masks or lab coats, as shown in Fig.12A, which enables non-invasive health diagnostics.[122] Moreover, the dynamic response curves of the sensor to different concentrations of C_3H_6O are shown in Fig.12B along with its response under light illumination, selectivity to interfering gases, and repeatability. However, maintaining consistent optical access and reduced power consumption remain as primary challenges that need to be addressed.

While integrating light sensors, optical access, and light-area geometry are very important in the sensor performance. To have good reproducibility in signals, especially in encapsulated devices, homogeneous illumination is to be maintained. Device encapsulation should take care

of the required light transmission along with stability against environmental factors like humidity, contamination, and stress due to mechanical deformations. These considerations apply uniquely to light-based sensors and are usually not relevant to thermally activated systems.[123,124]

Industrial IoT deployments further demonstrate scalability. Kim et al. integrated SnO_2-based VOC sensors into factory HVAC systems, achieving sub-ppm detection of benzene and toluene with edge-AI for predictive maintenance. Real-time data fusion with occupancy sensors and ventilation controls reduced worker exposure by 78% during chemical processing operations. In smart agriculture, flexible 2D material sensors (MoS_2/WSe_2 heterojunctions) embedded in crop-monitoring drones detect plant stress VOCs (e.g., methanol, hexanal) at 50 ppb, triggering automated irrigation via satellite-linked IoT networks to prevent yield losses exceeding 20%.[125]

Table 5. Comparative Evaluation of Nanocomposite Materials and Performance in Light-Activated Room-Temperature Gas Sensors

Materials	**Technique**	**Gases sensed**	**Concentration (ppm)**	**Operating Temperature (°C)**	**Band gap (eV)**	**Light source**	**Power / Intensity**	**Distance from light source to sensor**	**Surface area (m^2/g)**	**LOD**	**Response**	**Response/ Recovery times (s)**	**References**
ZnO-NiO	Solvothermal	Ethanol	100	125 (HT)	3.04	UV LED (365 nm)	1 mW/cm^2	10cm	230.54	102 ppb	3.1	56/16	114
CuO-TiO_2	Hydrothermal-Anodization	H_2S	100	25 (RT)	1.35-3.2	UV& Visible LED (365, 465, 525,	3W / 40 mW/cm^2	Varied to provide intenity in the	NA	3 ppm	46.81 %	41/92	113

View Article Online
DOI: 10.1039/D6NA00239K

						625 nm)		range of 17−48 mW/cm^2					
SnO_2-ZnO	Template-assisted hydrothermal	Formaldehyde	1-100	# (RT)	3.6-3.37	UV LED (365 nm)	2 mW	NA	NA	1.91 ppb	NA	36/76	126
FTO/ZnO/CuI/Au	Spin-coating	n-butylamine	150	# (RT)	3.23-3.02	UV lamp-365nm	5 mW/cm^2	NA	NA	6 ppm	18%	48/130	127
B-TiO_2/CuS	Hydrothermal	Acetone	20	25 (RT)	2.6	Visible light (Red LED: 610-620 nm); Yellow light: 580-590 nm;Bleu LED:	NA	3 cm	113.4	912 ppb	15.8 %	5.2/11.6	128

						440-450 nm)							
SnO_2/ ZnO	Electrospinning	Formaldehyde	50	25 (RT)	3.6-3.37	UV (365nm)	68 mW	1 cm	NA	NA	2.3%	NA	129
SnO_2/ TiO_2	Thermal evaporation-ALD	Formaldehyde	0.1	27 (RT)	3.6-3.2	UV LED (365 nm)	50 $\mu W/cm^2$	NA	74 (SnO)	0.1 ppm	15%	13/39	130
ZnO/ MoS_2	Hydrothermal	Acetone	20	30 (RT)	3.37-1.89	UV (375 nm)	50 $\mu W/cm^2$	NA	38.83	0.1 ppm	4.67	56/69	131
Zn_2SnO_4/SnO_2	Hydrothermal	TEA	75	# (RT)	3.6-3.9	UV (365 nm)	7.73 mW/cm^2	NA	NA	1 ppm	4.12	4/20	132
Tb_2O_3 /ZnO	Solvothermal	Acetic acid	100	20 (RT)	3.8-3.37	UV (365 nm)	8.31 mW/cm^2	NA	12.56	500 ppb	41.57 (sensitivity)	10/12	133
TiO2/ Yttria-Stabilized Zirconia (YSZ)	Electrospinning-ALD	Acetone	50	# (RT)	3.13-3.30	Visible light-Xenon lamp (300-450 nm)	100W / 146.3 mW/cm^2	5 cm	NA	0.15 ppm	4.8	NA	122

SnO_2-Graphene oxide	Hummers' method	Ethanol/ Ethylbenzene/acetone	1	25 (RT)	32:1 SnO_2-GO = 3.4; 4:1 SnO_2-GO= 3	LCS-100 Series Small area solar simulator (312 nm)	1.5 µW/cm^2	NA	32:1 SnO_2-GO =55; 4:1 SnO_2-GO=29	100 ppb	32:1 SnO_2-GO (EtOH response =2) 4:1 SnO_2-GO (EtOH response=0.006)	175/200	55
In_2O_3-functionalized graphene oxide	Hummers' method-solution based technique	Formaldehyde	0.5	# (RT)	2.38	Visible LED light (400-500 nm)	1 mW/cm^2	NA	NA	5 ppb	2.4	119/179	134
In_2O_3-ZnO	Hydrothermal	Formaldehyde	100	# (RT)	2.56-3.37	Xenon lamp (460nm)	500W /0.213 mW/cm^2	NA	NA	NA	419	NA/ < 30 s	135
NiO-ZnO	Flame spray	Acetone/	0.1	30 (RT)	3.2	AM1.5 Solar	67 mW/cm^2	NA	NA	0.01	0.77 (responsivity)	NA	89

	pyrolysis	Ethanol				Simulator				ppm			
NiO/Ag/$ZnIn_2S_4$	Hydrothermal-Photodeposition	Triethylamine	100	25 (RT)	2.58-2.64	White light LED	1.324×10^{-3} mW/cm^2	NA	95.7655	447 ppb	40	274/1166	117
In_2S_3/In_2O_3 with Pd/Pt/Au decoration	Chemical vapour deposition (CVD)	NO_2/Ethanol/Ammonia	50 (Ethanol)	25 (RT)	2.08-3.48	Blue light LED (450-455 nm)	12.0 mW/cm^2	2 cm	NA	NA	20%	372/214	136

 # Literatures where the specific room temperature values were not reported

Similar self-powered UV-activated photovoltaic sensing was reported by Rekha et al. using a ZnO/CuI heterojunction-based sensor for detecting n-butylamine under 365 nm illumination at an intensity of 1.3 mW cm^{-2}.[127] The merging of LED indicators with wireless connectivity demonstrates the feasibility of using light-activated sensors for practical monitoring.

In chemical manufacturing, AI-enhanced electronic noses combining hematite nanomaterials with IoT backhaul provide real-time VOC classification. Abdelghani et al. reported SnO_2-Y_2O_3 networks detecting H_2S at 10 ppm (318% response gain under UV) with DFT-validated adsorption, integrated into factory SCADA systems for leak localization and emergency shutdowns. [137,138] Urban industrial parks exploit volume-to-mass VOC conversion via IoT networks; recent deployments convert ppb readings to µg/m³ equivalents with <5% error, feeding regulatory dashboards and triggering zone-specific evacuations during exceedances. Chrome plating industries benefit from real-time IoT-AI systems monitoring VOC emissions with integrated forecasting. Ramadan et al. deployed multi-parameter sensor arrays

View Article Online
DOI: 10.1039/D6NA00239K

(temperature, humidity, VOC) linked to cloud dashboards, achieving 95% prediction accuracy for pollution spikes and triggering automated scrubber activation, which cut regulatory non-compliance by 67% in continuous operation.[139] For construction sites, IoT-enabled VOC sensors in ventilation systems continuously track indoor concentrations, automatically adjusting air exchange rates when thresholds are exceeded, maintaining worker safety during VOC-intensive painting and adhesive applications.[84]

Smart packaging represents another frontier, where near-field communication (NFC)-enabled VOC sensors in food containers monitor spoilage indicators like ethylene and amines. Pargoletti et al.'s GO-SnO_2 composites integrated into polymer films change colour upon 100 ppb ethanol detection, communicating shelf-life status to supply chain blockchain platforms and consumer apps, reducing food waste by 15-25% in perishable logistics. For urban air quality, wearable sensor networks deployed in public transit integrate with city dashboards; Liu et al.'s graphene-enhanced SMO arrays in bus-stop kiosks provide hyper-local VOC mapping (1 ppb formaldehyde resolution) with 5G backhaul for traffic-adaptive pollution alerts.[140]

Collectively, these developments showcase a paradigm shift from standalone sensing elements to intelligent, connected systems that merge materials innovation, miniaturized hardware, and IoT frameworks. The convergence holds great promise for revolutionary applications in the areas of health diagnostics, industrial safety, environmental monitoring, and logistics in the food industry, thereby defining the future of smart automated VOC sensing.

Although these integrated VOC sensor platforms have shown great progress in their translation from lab to field, there are still some challenges that need to be overcome for their widespread adoption, such as stability in harsh environments, suppression of cross-sensitivity, and interoperability in IoT. The Future Perspectives and Outlook section of this review article synthesizes these advances and provides strategic directions for the future, including materials innovation, AI-assisted data fusion, regulatory harmonization, and commercialization plans to unlock the full potential of light-activated SMO heterojunction sensors in smart ecosystems.

View Article Online
DOI: 10.1039/D6NA00239K

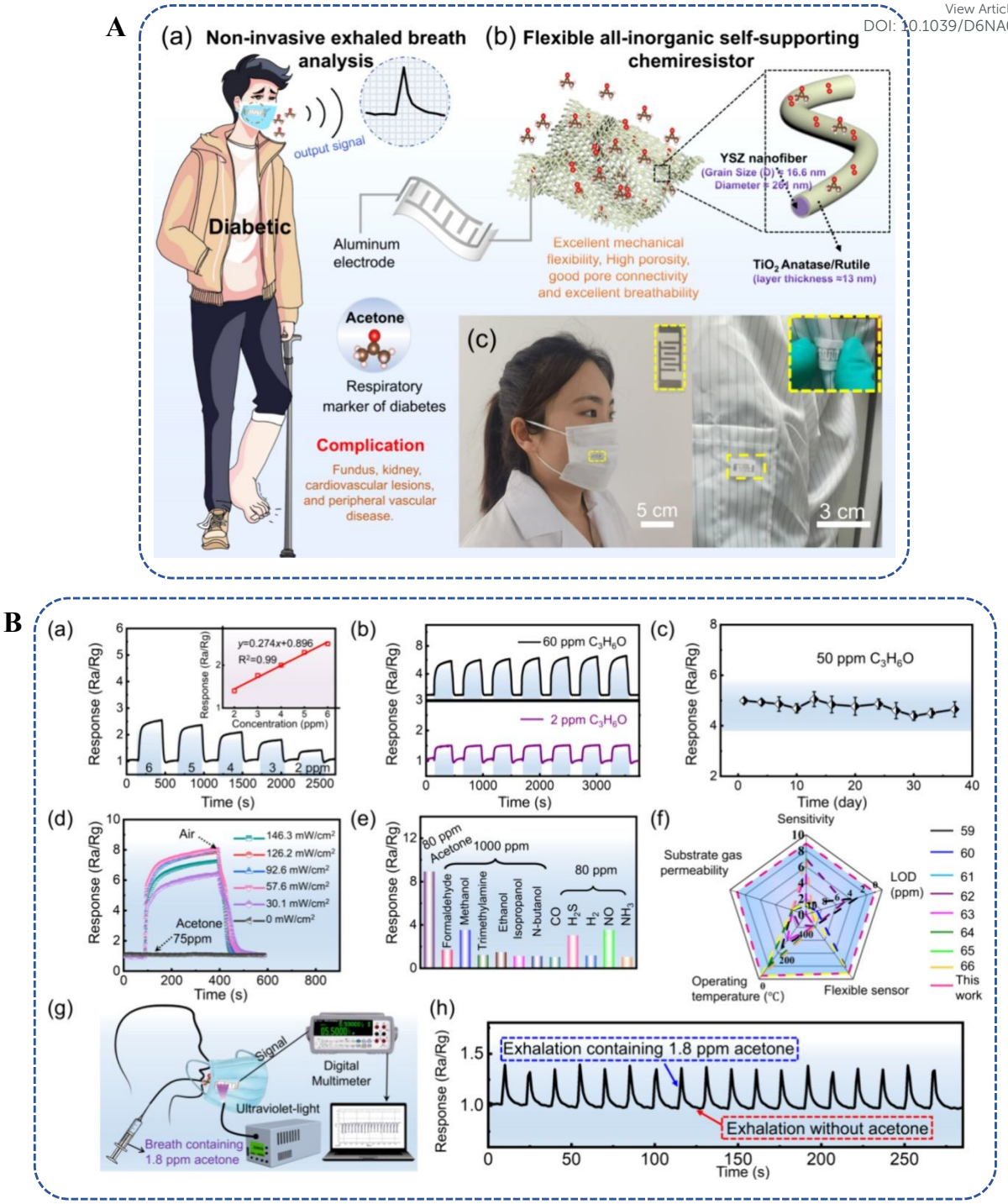

Fig.12A *(a)* Schematic representation of non-invasive approach for diabetes diagnosis. (b) Schematic diagram showing flexible all-inorganic chemiresistors. *(c)* demonstration of the sensor's excellent compatibility with masks and lab coats for wearable applications.[122]

Fig.12B *(a)* Dynamic sensing response profiles of the YSZ/TiO2-A/R gas sensor to low concentrations of C_3H_6O (2ppm to 6ppm). *(b)* Reproducibility of the YSZ/TiO_2-A/R gas sensor response to 60 and 2 ppm C_3H_6O measured at room temperature under UV

View Article Online
DOI: 10.1039/D6NA00239K

illumination. *(c)* 37 days stability studies. *(d)* Response of the sensor to 75 ppm of C_3H_6O under different UV light intensities, and *(e)* selectivity studies in exhaled breath for the YSZ/TiO_2-A/R gas sensor. *(f)* Comparison of the performance metric of the YSZ/TiO_2-A/R gas sensor with those of existing C_3H_6O sensors *(g)*. Flowchart for simulated diabetic breath testing. *(h) R*epeatability studies of the YSZ/TiO_2-A/R sensor for simulating diabetic breath signals. Reprinted from ACS sensors, Vol 10, Wanying Cheng, Xiaowei Li, Chaohan Han, Yu Liu, Aoqun Xue, Haipeng Dong, Xinghua Li, Changlu Shao, Yichun Liu, Room-Temperature Wearable Chemiresistor Based on a Flexible Inorganic Photoactive Anatase–Rutile TiO_2/Yttria-Stabilized Zirconia Nanofiber Network, Copyrights (2025) with permission from ACS.[122]

5. Future Perspectives and Outlook

Room-temperature VOC sensors have received comparatively little attention due to the thermal activation requirements of most sensing materials, yet next-generation smart cities, wearables, and IoT platforms demand ambient-condition operation without compromising safety or reliability. While porous heterostructures offer high surface-to-volume ratios for enhanced gas adsorption, persistent challenges include material brittleness, biocompatibility limitations, suboptimal light responsiveness, and thermal endurance constraints that hinder flexible, real-time deployment.[125,141]

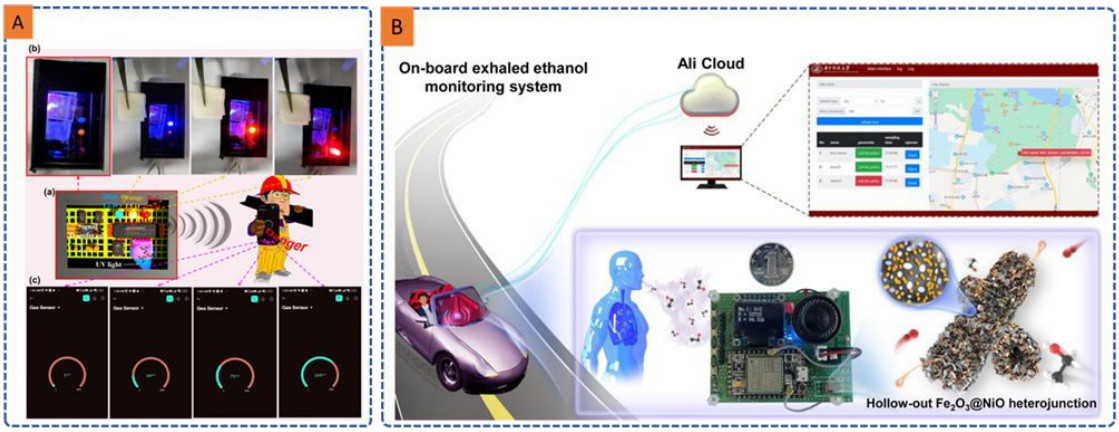

Fig.13 A (a) Schematic diagram of the TEA sensor prototype showing signal processing and wireless communication to the employee's smartphone; (b) response of the sensor to TEA by bringing TEA-soaked tissue paper near the sensing element to allow adsorption of TEA molecules on the sensor surface; and (c)wirelessly transmitted signals displayed on the employee's smartphone.[120] Reprinted from ACS sensors, Vol 9, Rahul Suresh Ghuge, Sreelakshmi Madhavanunni Rekha, Hajeesh Kumar Vikraman, Surya Velappa Jayaraman, Mangalampalli S R N Kiran, S Venkataprasad Bhat, Yuvaraj Sivalingam, Transparent

TiO_2/MoO_3 Heterojunction-Based Photovoltaic Self-Powered Triethylamine Gas Sensor with IoT-Enabled Smartphone Interface, Copyrights (2024) with permission from ACS Fig. 13B An intelligent, IoT-enabled integrated system for monitoring drunk driving. Reprinted from Applied Materials & Interfaces, Vol 15, Long Li, Licheng Zhou, Zhixiang Hu, Tiankun Li, Bingbing Chen, Hua-Yao Li, Huan Liu, Hollow-Out Fe_2O_3-Loaded NiO Heterojunction Nanorods Enable Real-Time Exhaled Ethanol Monitoring under High Humidity, Copyrights (2025) with permission from ACS.[121]

Light activation emerges as a compelling alternative to thermal energy, circumventing microheater costs, material degradation, and explosion risks with flammable VOCs. However, sunlight-dependent performance falters in low-insolation regions—high-latitude areas (northern Canada, Scandinavia, Siberia), persistently cloudy zones (UK, Pacific Northwest), shaded urban canyons, and dense rainforests, necessitating robust indoor/visible-light solutions.[140] Future research on sensors needs to prioritize the real RT operation, obviating the need for external heating, to distinguish from the current LT operation.

- **Materials Innovation:** Self-healing MXene, polymers, and perovskite hybrid structures with intrinsic self-rejuvenating properties, can detect various VOCs at the sub-ppb level while providing more than ten times improvement in humidity stability. Moreover, the high biocompatibility of the sensing structures can be seamlessly integrated with the human body. The Machine Learning-based sensing platforms can improve the performance of wearable sensors by providing the capability for room-temperature operation, reducing the power requirements, and effectively eliminating interference from other gases.[125,141]
- **Device Miniaturization and Energy Autonomy:**

  Wireless IoT sensor covering homes, offices, and smart cities envisions the light-activated SMO heterojunction as a key enabling technology for environmental conservation, merging material science and digital ecosystems to protect global health and sustainability.

With the ever-increasing pace of technological advancements, AI-based wireless IoT sensor networks are growing rapidly, especially in the context of smart cities. In the next decade, the increasing capabilities of technology and the need for cleaner and safer environments will trigger widespread adoption for continuous environmental surveillance in living spaces, work environments, and industrial settings. Highly adaptable, miniaturized, and energy-efficient IoT sensors fuelled by renewable energy sources will enable real-time air quality analysis and leak

View Article Online
DOI: 10.1039/D6NA00239K

detection, ensuring industrial and public health and safety. The intersection of these makes light-activated SMO heterojunctions the foundational technology for the intelligent sensing age, integrating materials science and digital transformation to secure healthy, sustainable, and protected environments through sustainable management.[125,142]

To achieve this vision, there is a pressing need for interdisciplinary collaboration between materials science, photonics, AI, and systems engineering to address the current challenges in scalability and standardization. The path from laboratory prototypes to real-time sensor fabrics holds not only technological promise but also immense social value. mitigating VOC-related morbidity, improving workplace safety, and facilitating precision environmental governance globally. Light-activated SMO heterojunctions will continue to play a pivotal role in redefining intelligent sensing, converting invisible chemical hazards into valuable intelligence for sustainable futures.

Conclusions

This review has comprehensively analysed the developments in semiconductor metal oxide heterojunction-based sensors for the detection of volatile organic compounds, focusing on light-activated mechanisms to address the limitations of traditional sensing approaches. The combination of heterojunction engineering and photoactivation significantly improves the sensitivity, selectivity, and robustness of the sensors, allowing for operation at lower temperatures and shorter response times, which are essential for practical applications. Although considerable progress has been made, there are still challenges to be addressed in terms of long-term stability under different humidity conditions, cross-sensitivity, and the scalability of the fabrication process for commercialization. The coupling of these sensing technologies with wearable, IoT, and smart packaging systems holds revolutionary potential for transformative applications in environmental monitoring, food security, and non-invasive medical diagnostics. Future research efforts should be directed towards the development of innovative hybrid materials, flexible sensor configurations, and data-driven strategies using artificial intelligence to develop adaptive and robust sensing solutions. A collaborative approach to innovation at the intersection of materials science, device engineering, and data science will be crucial to unlock the full potential of these emerging technologies. This review provides a starting point and motivation for continued innovation towards next-generation VOC sensors that can address the challenges of sustainability, accuracy, and applicability to different societal needs.

View Article Online
DOI: 10.1039/D6NA00239K

Authors contributions

Phibakordor Shnagpliang: Conceptualization, Data curation, Formal analysis, Investigation, Writing – original draft. **Suresh D. Kulkarni**: Formal analysis, Validation, Writing – review & editing. **Suraj Sunil Joshi**: Formal analysis, Data curation, and Investigation. **K.S. Choudhari**: Conceptualization, Formal analysis, Supervision, Writing – review & editing.

Conflicts of interest

The authors have no known competing financial interests or personal relationships that could have appeared to influence the work reported in this paper.

Data availability

No new data have been generated in this review.

Acknowledgements

Ms. Phibakordor Shangpliang and Mr. Suraj Sunil Joshi would like to thank Manipal Academy of Higher Education (MAHE), Manipal, for the financial support provided through the Dr. T. M. A. fellowship.

References

1. Gorokh G, Zakhlebayeva A, Taratyn I, Lozovenko A, Zhylinski V, Iji M, et al. A Micropowered Chemoresistive Sensor Based on a Thin Alumina Nanoporous Membrane and Snx Bik Moy Oz Nanocomposite. Sensors. 2022;22(10). doi:10.3390/s22103640
2. Dhall S, Mehta BR, Tyagi AK, Sood K. A review on environmental gas sensors: Materials and technologies. Sensors International. 2021. doi:10.1016/j.sintl.2021.100116
3. Hoa ND, Duy N Van, El-Safty SA, Hieu N Van. Meso-/nanoporous semiconducting metal oxides for gas sensor applications. Journal of Nanomaterials. 2015. doi:10.1155/2015/972025
4. Han B, Rupam TH, Chakraborty A, Saha BB. A comprehensive review on VOCs sensing using different functional materials: Mechanisms, modifications, challenges and opportunities. Renewable and Sustainable Energy Reviews. 2024. doi:10.1016/j.rser.2024.114365
5. Manisalidis I, Stavropoulou E, Stavropoulos A, Bezirtzoglou E. Environmental and Health Impacts of Air Pollution: A Review. Frontiers in Public Health. 2020. doi:10.3389/fpubh.2020.00014
6. Van Tran V, Park D, Lee YC. Indoor air pollution, related human diseases, and recent trends in the control and improvement of indoor air quality. International Journal of Environmental Research and Public Health. 2020. doi:10.3390/ijerph17082927

7. Khoshakhlagh AH, Mohammadzadeh M, Manafi SS, Yousefian F, Gruszecka-Kosowska A. Inhalational exposure to formaldehyde, carcinogenic, and non-carcinogenic risk assessment: A systematic review. Environmental Pollution. Elsevier Ltd; 2023. doi:10.1016/j.envpol.2023.121854 PubMed PMID: 37236589.

8. Zhou X, Zhou X, Wang C, Zhou H. Environmental and human health impacts of volatile organic compounds: A perspective review. Chemosphere. 2023 Feb 1;313. doi:10.1016/j.chemosphere.2022.137489 PubMed PMID: 36513206.

9. Gallego E, Perales JF, Calaf JM. Continuous monitoring of volatile organic compounds through sensorization. Automatic sampling during pollution/odour/nuisance episodic events. Atmos Environ. 2023 Apr 15;299. doi:10.1016/j.atmosenv.2023.119657

10. Epping R, Koch M. On-Site Detection of Volatile Organic Compounds (VOCs). Molecules. MDPI; 2023. doi:10.3390/molecules28041598 PubMed PMID: 36838585.

11. Jalal AH, Alam F, Roychoudhury S, Umasankar Y, Pala N, Bhansali S. Prospects and Challenges of Volatile Organic Compound Sensors in Human Healthcare. ACS Sensors. American Chemical Society; 2018. p. 1246–63. doi:10.1021/acssensors.8b00400 PubMed PMID: 29879839.

12. Xu K, Wu K, Xu J, Planche MP, Deng S, Liao H, et al. Metal oxide semiconductor-based heterojunctions synthesized by wet-chemical strategies for efficient volatile organic compounds detection. Coordination Chemistry Reviews. Elsevier B.V.; 2025. doi:10.1016/j.ccr.2025.216735

13. Li B, Zhou Q, Peng S, Liao Y. Recent Advances of SnO2-Based Sensors for Detecting Volatile Organic Compounds. Frontiers in Chemistry. Frontiers Media S.A.; 2020. doi:10.3389/fchem.2020.00321

14. Postica V, Vahl A, Santos-Carballal D, Dankwort T, Kienle L, Hoppe M, et al. Tuning ZnO Sensors Reactivity toward Volatile Organic Compounds via Ag Doping and Nanoparticle Functionalization. ACS Appl Mater Interfaces. 2019 Aug 28;11(34):31452–66. doi:10.1021/acsami.9b07275 PubMed PMID: 31333012.

15. Srivastava S, Pandey NK, Verma V, Singh P, Verma A, Yadav N, et al. Development of highly sensitive SnO2@ZnO based chemiresistor for Ammonia sensing. Mater Chem Phys. 2024 Feb 1;313. doi:10.1016/j.matchemphys.2023.128775

16. Liu L, Wang Y, Liu Y, Wang S, Li T, Feng S, et al. Heteronanostructural metal oxide-based gas microsensors. Microsystems and Nanoengineering. Springer Nature; 2022. doi:10.1038/s41378-022-00410-1

17. Nasriddinov A, Zairov R, Rumyantseva M. Light-activated semiconductor gas sensors: pathways to improve sensitivity and reduce energy consumption. Frontiers in Chemistry. 2025. doi:10.3389/fchem.2025.1538217

18. David E, Niculescu VC. Volatile organic compounds (Vocs) as environmental pollutants: Occurrence and mitigation using nanomaterials. International Journal of Environmental Research and Public Health. 2021. doi:10.3390/ijerph182413147

19. Lawaniya SD, Awasthi A, Menezes PW, Awasthi K. Detection of Foodborne Pathogens Through Volatile Organic Compounds Sensing via Metal Oxide Gas Sensors. Advanced Sensor Research. 2025 Jan;4(1). doi:10.1002/adsr.202400101

20. Horvat T, Pehnec G, Jakovljević I. Volatile Organic Compounds in Indoor Air: Sampling, Determination, Sources, Health Risk, and Regulatory Insights. Toxics. Multidisciplinary Digital Publishing Institute (MDPI); 2025. doi:10.3390/toxics13050344

21. Zhao D, Yang Y, Tham YJ, Zou S. Emission of marine volatile organic compounds (VOCs) by phytoplankton— a review. Marine Environmental Research. Elsevier Ltd; 2023. doi:10.1016/j.marenvres.2023.106177 PubMed PMID: 37741052.

22. Yadav R, Sahu LK, Tripathi N, Pal D, Beig G, Jaaffrey SNA. Investigation of emission characteristics of NMVOCs over urban site of western India. Environmental Pollution. 2019 Sep 1;252:245–55. doi:10.1016/j.envpol.2019.05.089 PubMed PMID: 31153029.

23. Fu X. Indoor Microbial Volatile Organic Compound (MVOC) Levels and Associations with Respiratory Health, Sick Building Syndrome (SBS), and Allergy. In: Environmental Mycology in Public Health: Fungi and Mycotoxins Risk Assessment and Management. 2015. doi:10.1016/B978-0-12-411471-5.00022-3

24. Sahlberg B, Gunnbjörnsdottir M, Soon A, Jogi R, Gislason T, Wieslander G, et al. Airborne molds and bacteria, microbial volatile organic compounds (MVOC), plasticizers and formaldehyde in dwellings in three North European cities in relation to sick building syndrome (SBS). Science of the Total Environment. 2013 Feb 1;444:433–40. doi:10.1016/j.scitotenv.2012.10.114 PubMed PMID: 23280302.

25. Misztal PK, Lymperopoulou DS, Adams RI, Scott RA, Lindow SE, Bruns T, et al. Emission Factors of Microbial Volatile Organic Compounds from Environmental Bacteria and Fungi. Environ Sci Technol. 2018 Aug 7;52(15):8272–82. doi:10.1021/acs.est.8b00806 PubMed PMID: 29947506.

26. Wang H, Liu X, Wu C, Lin G. Regional to global distributions, trends, and drivers of biogenic volatile organic compound emission from 2001 to 2020. Atmos Chem Phys. 2024;24(5). doi:10.5194/acp-24-3309-2024

27. Moura PC, Raposo M, Vassilenko V. Breath volatile organic compounds (VOCs) as biomarkers for the diagnosis of pathological conditions: A review. Biomedical Journal. 2023. doi:10.1016/j.bj.2023.100623

28. Liu Z, Wang M, Wu M, Li X, Liu H, Niu N, et al. Volatile organic compounds (VOCs) from plants: From release to detection. TrAC - Trends in Analytical Chemistry. Elsevier B.V.; 2023. doi:10.1016/j.trac.2022.116872

29. Luo R, Lun X, Gao R, Wang L, Yang Y, Su X, et al. A Review of Biogenic Volatile Organic Compounds from Plants: Research Progress and Future Prospects. Toxics. Multidisciplinary Digital Publishing Institute (MDPI); 2025. doi:10.3390/toxics13050364

30. Sekimoto K, Coggon MM, Gkatzelis GI, Stockwell CE, Peischl J, Soja AJ, et al. Fuel-Type Independent Parameterization of Volatile Organic Compound Emissions from Western US Wildfires. Environ Sci Technol. 2023 Sep 5;57(35):13193–204. doi:10.1021/acs.est.3c00537 PubMed PMID: 37611137.

31. Zuo Z. Why algae release volatile organic compounds - The emission and roles. Frontiers in Microbiology. Frontiers Media S.A.; 2019. doi:10.3389/fmicb.2019.00491

32. Alford KL, Kumar N. Pulmonary health effects of indoor volatile organic compounds—a meta-analysis. Int J Environ Res Public Health. 2021 Feb 2;18(4):1–12. doi:10.3390/ijerph18041578 PubMed PMID: 33562372.

33. Substances Listed in the Fifteenth Report on Carcinogens Bold entries indicate new or changed listings in the Fifteenth Report on Carcinogens [Internet]. Available from: http://ntp.niehs.nih.gov/go/roc

34. Report on Carcinogens, Fifteenth Edition [Internet]. Available from: http://toxnet.nlm.nih.gov/

35. Saeedi M, Malekmohammadi B, Tajalli S. Interaction of benzene, toluene, ethylbenzene, and xylene with human's body: Insights into characteristics, sources and health risks. Journal of Hazardous Materials Advances. Elsevier B.V.; 2024. doi:10.1016/j.hazadv.2024.100459

36. Protano C, Buomprisco G, Cammalleri V, Pocino RN, Marotta D, Simonazzi S, et al. The carcinogenic effects of formaldehyde occupational exposure: A systematic review. Cancers. MDPI; 2022. doi:10.3390/cancers14010165

37. Vijayraghavan S, Porcher L, Mieczkowski PA, Saini N. Acetaldehyde makes a distinct mutation signature in single-stranded DNA. Nucleic Acids Res. 2022 Jul 22;50(13):7451–64. doi:10.1093/nar/gkac570 PubMed PMID: 35776120.

38. Montero-Montoya R, López-Vargas R, Arellano-Aguilar O. Volatile organic compounds in air: Sources, distribution, exposure and associated illnesses in children. Annals of Global Health. Levy Library Press; 2018. p. 225–38. doi:10.29024/aogh.910 PubMed PMID: 30873816.

39. Hussain MS, Gupta G, Mishra R, Patel N, Gupta S, Alzarea SI, et al. Unlocking the secrets: Volatile Organic Compounds (VOCs) and their devastating effects on lung cancer. Pathology Research and Practice. Elsevier GmbH; 2024. doi:10.1016/j.prp.2024.155157 PubMed PMID: 38320440.

40. Li S, Liao X, Ma R, Deng N, Wu H, Zhang Z, et al. Effects of Co-Exposure to Benzene, Toluene, and Xylene, Polymorphisms of microRNA Genes, and Their Interactions on Genetic Damage in Chinese Petrochemical Workers. Toxics. 2024 Nov 1;12(11). doi:10.3390/toxics12110821

41. Li XB, Yuan B, Huangfu Y, Yang S, Song X, Qi J, et al. Vertical changes in volatile organic compounds (VOCs) and impacts on photochemical ozone formation. Atmos Chem Phys. 2025 Feb 26;25(4):2459–72. doi:10.5194/acp-25-2459-2025

42. Guenther AB, Jiang X, Heald CL, Sakulyanontvittaya T, Duhl T, Emmons LK, et al. The model of emissions of gases and aerosols from nature version 2.1 (MEGAN2.1): An extended and updated framework for modeling biogenic emissions. Geosci Model Dev. 2012;5(6):1471–92. doi:10.5194/gmd-5-1471-2012

43. Chen K, Hamilton C, Ries B, Lum M, Mayorga R, Tian L, et al. Relative Humidity Modulates the Physicochemical Processing of Secondary Brown Carbon Formation from Nighttime Oxidation of Furan and Pyrrole. ACS ES&T Air. 2024 May 10;1(5):426–37. doi:10.1021/acsestair.4c00025

44. Acharya S, Sharmin RS, Fiutowski J, Mishra YK, de Oliveira Hansen R. Sensing volatile organic compounds in aquatic samples: a review. Water Supply. IWA Publishing; 2024. p. 3314–25. doi:10.2166/ws.2024.224

45. Jing D, Yang K, Shi Z, Cai X, Li S, Li W, et al. Novel approach for identifying VOC emission characteristics based on mobile monitoring platform data and deep learning: Application of source apportionment in a chemical industrial park. Heliyon. 2024 Apr 30;10(8). doi:10.1016/j.heliyon.2024.e29077

46. Mirzaei A, Leonardi SG, Neri G. Detection of hazardous volatile organic compounds (VOCs) by metal oxide nanostructures-based gas sensors: A review. Ceramics International. Elsevier Ltd; 2016. p. 15119–41. doi:10.1016/j.ceramint.2016.06.145

47. Zhang C, Qian L, Zeng W. MOS based gas sensor in detection of volatile organic compounds: A review. Sensors and Actuators A: Physical. Elsevier B.V.; 2025. doi:10.1016/j.sna.2025.116818

48. Tian J, Zhang Q, Peng M, Guo L, Zhao Q, Lin W, et al. Exhaled volatile organic compounds as novel biomarkers for early detection of COPD, asthma, and PRISm: a cross-sectional study. Respir Res. 2025 Dec 1;26(1). doi:10.1186/s12931-025-03242-5 PubMed PMID: 40325477.

49. Sørensen SB, Kristensen K. Low-cost sensor-based investigation of CO2 and volatile organic compounds in classrooms: Exploring dynamics, ventilation effects and perceived air quality relations. Build Environ. 2024 Apr 15;254. doi:10.1016/j.buildenv.2024.111369

50. Jia Z, Patra A, Kutty VK, Venkatesan T. Critical review of volatile organic compound analysis in breath and in vitro cell culture for detection of lung cancer. Metabolites. MDPI AG; 2019. doi:10.3390/metabo9030052

51. Info_Note_MOX_sensor.

52. Jayan H, Zhou R, Sun C, Wang C, Yin L, Zou X, et al. Intelligent Gas Sensors for Food Safety and Quality Monitoring: Advances, Applications, and Future Directions. Foods. Multidisciplinary Digital Publishing Institute (MDPI); 2025. doi:10.3390/foods14152706

53. Nabaei SH, Lenfant R, Rajan VG, Chen D, Timko MP, Campbell B, et al. Detecting Plant VOC Traces Using Indoor Air Quality Sensors [Internet]. 2025 Apr 3. Available from: http://arxiv.org/abs/2504.03785

54. Ramadan KMA, Bendary ESA, Khalil HB, Ali SA, Ahmed AR, Mahmoud MAA. Smart Detection of Food Spoilage Using Microbial Volatile Compounds: Technologies, Challenges, and Future Outlook. Journal of agricultural and food chemistry. 2025. p. 19222–43. doi:10.1021/acs.jafc.5c05927 PubMed PMID: 40717620.

55. Pargoletti E, Hossain UH, Di Bernardo I, Chen H, Tran-Phu T, Chiarello GL, et al. Engineering of SnO2-Graphene Oxide Nanoheterojunctions for Selective Room-Temperature Chemical Sensing and Optoelectronic Devices. ACS Appl Mater Interfaces. 2020;12(35). doi:10.1021/acsami.0c09178

56. Liu D, Qian J, Chen M, Wang K, An L, Pan L, et al. Novel in-situ embedded SnO2-ZnO heterojunction for highly sensitive and selective gas sensors for lung cancer screening applications. Chemical Engineering Journal. 2025 May 15;512. doi:10.1016/j.cej.2025.162681

57. Lin H, Jiang H, Adade SYSS, Kang W, Xue Z, Zareef M, et al. Overview of advanced technologies for volatile organic compounds measurement in food quality and safety. Critical Reviews in Food Science and Nutrition. 2023. doi:10.1080/10408398.2022.2056573

58. Okechukwu VO, Njobeh PB, Kappo AP, Mamo MA. Room temperature detection of aspergillus flavus volatile organic compounds (VOCs) under simulated conditions using graphene oxide and tin oxide Nanorods (SnO2 NRs-GO). Food Chem. 2024 Oct 30;456. doi:10.1016/j.foodchem.2024.140068 PubMed PMID: 38878549.

59. Spinelle L, Gerboles M, Kok G, Persijn S, Sauerwald T. Review of portable and low-cost sensors for the ambient air monitoring of benzene and other volatile organic compounds. Sensors (Switzerland). 2017. doi:10.3390/s17071520

60. Zeki ÖC, Eylem CC, Nemutlu E. Optimization of GC-MS run time for untargeted metabolomics: Trade-offs between speed, coverage, and repeatability. J Pharm Biomed Anal. 2025 Dec 15;266. doi:10.1016/j.jpba.2025.117068 PubMed PMID: 40743981.

61. Xia L, Liu Y, Chen RT, Weng B, Zou Y. Advancements in miniaturized infrared spectroscopic-based volatile organic compound sensors: A systematic review. Applied Physics Reviews. American Institute of Physics; 2024. doi:10.1063/5.0197236

62. Xiao Y, Li H, Wang C, Pan S, He J, Liu A, et al. Room Temperature Wearable Gas Sensors for Fabrication and Applications. Advanced Sensor Research. 2024;3(3). doi:10.1002/adsr.202300035

63. Wang J, Deng H, Li X, Yang C, Xia Y. Visible-light photocatalysis enhanced room-temperature formaldehyde gas sensing by MoS2/rGO hybrids. Sens Actuators B Chem. 2020;304. doi:10.1016/j.snb.2019.127317

64. Kumar R, Liu X, Zhang J, Kumar M. Room-Temperature Gas Sensors Under Photoactivation: From Metal Oxides to 2D Materials. Nano-Micro Letters. Springer; 2020. doi:10.1007/s40820-020-00503-4

65. Lopis AD, Choudhari KS, Sai R, Kanakikodi KS, Maradur SP, Shivashankar SA, et al. Laddered type-1 heterojunction: Harvesting full-solar-spectrum in scavenger free photocatalysis. Solar Energy. 2022 Jul 1;240:57–68. doi:10.1016/j.solener.2022.05.022

66. Lopis AD, Choudhari KS, Sai R, Sudarshana, Kanakikodi KS, Maradur SP, et al. Co2+-laddered heterojunction a next-generation solar-photocatalyst: Unusually improved activity for the decomposition of pharmaceuticals, dyes, and microplastics. Mater Res Bull. 2024 Aug 1;176. doi:10.1016/j.materresbull.2024.112836

67. Qiao S, Di M, Jiang JX, Han BH. Conjugated porous polymers for photocatalysis: The road from catalytic mechanism, molecular structure to advanced applications. EnergyChem. 2022. doi:10.1016/j.enchem.2022.100094

68. Wang Y, Du K, Xu R, Cui D, Shi Y, Hao W, et al. Bismuth-based semiconductor heterostructures for photocatalytic pollution gases removal. Current Opinion in Green and Sustainable Chemistry. 2023. doi:10.1016/j.cogsc.2023.100824

69. Low J, Yu J, Jaroniec M, Wageh S, Al-Ghamdi AA. Heterojunction Photocatalysts. Advanced Materials. 2017. doi:10.1002/adma.201601694

70. Tang Y, Zhao Y, Liu H. Room-Temperature Semiconductor Gas Sensors: Challenges and Opportunities. ACS Sensors. American Chemical Society; 2022. p. 3582–97. doi:10.1021/acssensors.2c01142 PubMed PMID: 36399520.

71. Bulemo PM, Kim DH, Shin H, Cho HJ, Koo WT, Choi SJ, et al. Selectivity in Chemiresistive Gas Sensors: Strategies and Challenges. Chemical Reviews. American Chemical Society; 2025. p. 4111–83. doi:10.1021/acs.chemrev.4c00592 PubMed PMID: 40198852.

72. Dey A. Semiconductor metal oxide gas sensors: A review. Materials Science and Engineering: B. 2018. doi:10.1016/j.mseb.2017.12.036

73. Saruhan B, Lontio Fomekong R, Nahirniak S. Review: Influences of Semiconductor Metal Oxide Properties on Gas Sensing Characteristics. Frontiers in Sensors. 2021. doi:10.3389/fsens.2021.657931

74. Ganesh Moorthy S, Bouvet M. Effects of Visible Light on Gas Sensors: From Inorganic Resistors to Molecular Material-Based Heterojunctions. Sensors. 2024. doi:10.3390/s24051571

75. Suh JM, Sohn W, Shim YS, Choi JS, Song YG, Kim TL, et al. P-p Heterojunction of Nickel Oxide-Decorated Cobalt Oxide Nanorods for Enhanced Sensitivity and Selectivity toward Volatile Organic Compounds. ACS Appl Mater Interfaces. 2018 Jan 10;10(1):1050–8. doi:10.1021/acsami.7b14545 PubMed PMID: 29235841.

76. Khatib M, Haick H. Sensors for Volatile Organic Compounds. ACS Nano. 2022. doi:10.1021/acsnano.1c10827

77. Wang J, Shen H, Xia Y, Komarneni S. Light-activated room-temperature gas sensors based on metal oxide nanostructures: A review on recent advances. Ceramics International. 2021. doi:10.1016/j.ceramint.2020.11.187

78. De S, Venkataramani N, Prasad S, Dusane RO, Presmanes L, Thimont Y, et al. Ethanol and Hydrogen Gas-Sensing Properties of CuO-CuFe2O4 Nanostructured Thin Films. IEEE Sens J. 2018;18(17). doi:10.1109/JSEN.2018.2849330

79. De S, Venkataramani N, Prasad S, Dusane RO, Presmanes L, Thimont Y, et al. Ethanol and Hydrogen Gas-Sensing Properties of CuO-CuFe2O4 Nanostructured Thin Films. IEEE Sens J. 2018;18(17). doi:10.1109/JSEN.2018.2849330

80. Uma S, Shobana MK. Band structure and mechanism of semiconductor metal oxide heterojunction gas sensor. Inorganic Chemistry Communications. 2024. doi:10.1016/j.inoche.2023.111941

81. Ji H, Zeng W, Li Y. Gas sensing mechanisms of metal oxide semiconductors: A focus review. Nanoscale. Royal Society of Chemistry; 2019. p. 22664–84. doi:10.1039/c9nr07699a PubMed PMID: 31755888.

82. Saruhan B, Lontio Fomekong R, Nahirniak S. Review: Influences of Semiconductor Metal Oxide Properties on Gas Sensing Characteristics. Frontiers in Sensors. Frontiers Media SA; 2021. doi:10.3389/fsens.2021.657931

83. Chai H, Zheng Z, Liu K, Xu J, Wu K, Luo Y, et al. Stability of Metal Oxide Semiconductor Gas Sensors: A Review. IEEE Sensors Journal. Institute of Electrical and Electronics Engineers Inc.; 2022. p. 5470–81. doi:10.1109/JSEN.2022.3148264

84. Ghiai M, Pahlevani M. Enhancing Indoor Environmental Quality through IoT: A Review of Applications and Challenges. Journal of Information Technology in Construction. 2025 Sep 17;30(1):1478. doi:10.36680/j.itcon.2025.060

85. Ren H, Wan J, Pan H, Huang J. Facile synthesis of porous SnO2@CuO nanosheets with highly sensitive performance of VOCs. Mater Res Bull. 2025 May 1;185. doi:10.1016/j.materresbull.2025.113313

86. Sen S, Kundu S. Bio-waste derived reduced graphene oxide (rGO) decorated Cr (III) doped α-Fe2O3 nanocomposite for selective ppm-level acetone sensing at room temperature: Potential approach towards non-invasive diagnosis of diabetic biomarker. Adv Compos Hybrid Mater. 2025 Feb 1;8(1). doi:10.1007/s42114-025-01241-0

87. Li S, Xie L, He M, Hu X, Luo G, Chen C, et al. Metal-Organic frameworks-derived bamboo-like CuO/In2O3 Heterostructure for high-performance H2S gas sensor with Low operating temperature. Sens Actuators B Chem. 2020;310. doi:10.1016/j.snb.2020.127828

88. He T, Sun S, Huang B, Li X. MXene/SnS2 Heterojunction for Detecting Sub-ppm NH3 at Room Temperature. ACS Appl Mater Interfaces. 2023 Jan 25;15(3):4194–207. doi:10.1021/acsami.2c18097 PubMed PMID: 36631735.

89. Chen H, Bo R, Shrestha A, Xin B, Nasiri N, Zhou J, et al. NiO–ZnO Nanoheterojunction Networks for Room-Temperature Volatile Organic Compounds Sensing. Adv Opt Mater. 2018;6(22). doi:10.1002/adom.201800677

90. Jadhav GF, Al-Hejri TM, Suryawanshi RR, Shaikh SF, Mane RS, Palaniswami M, et al. Soft chemical synthesis of Bi2O3 tailored TiO2 heterostructure composites for enhanced VOC sensing at room-temperature. Ceram Int. 2025. doi:10.1016/j.ceramint.2025.08.078

91. Srinivasan P, Prakalya D, Jeyaprakash BG. UV-activated ZnO/CdO n-n isotype heterostructure as breath sensor. J Alloys Compd. 2020 Apr 5;819. doi:10.1016/j.jallcom.2019.152985

92. Liu M, Sun Q, Zhu Y, Hu P, Wu Z. Highly selective room-temperature formaldehyde gas sensor based on SnO2 nanoparticle-modified In2O3 microspheres. Appl Surf Sci. 2025 Jun 30;695. doi:10.1016/j.apsusc.2025.162856

93. Zhao Z, Dong Y, Meng X, Wu P, Wang J. W18O49/CeO2 heterojunction for enhanced n-Butanol gas sensor operating at room temperature. Ceram Int. 2025 Nov. doi:10.1016/j.ceramint.2025.11.027

94. Kumar R, Kumar Keshari A, Sinha Roy S, Patel G, Raju V, Sain S, et al. One-Step Solvothermally Synthesized Ni Doped MoS2@SnS2 Nanocomposite as a High Performance Supercapacitor Electrode Material. ChemNanoMat. 2025 Apr 1;11(4). doi:10.1002/cnma.202400584

95. Kumar S, Puri NK. Highly selective sustainable ethanol gas sensor based on p-p heterojunction of SnS/MoSe2 nanocomposite at room temperature. Mater Chem Phys. 2024 Oct 15;326. doi:10.1016/j.matchemphys.2024.129802

96. Hu D, Shao W, Chen L, Yang R, Huang S, Wang X, et al. Nanofiber-Structured SnO2/Co3O4 Modified Ta2O5 Heterojunction for Room-Temperature Ethanol Sensing. ACS Appl Nano Mater. 2024 Jun 28;7(12):14476–86. doi:10.1021/acsanm.4c01949

97. Kashyap A, Chakraborty B, Siddiqui MS, Tyagi H, Kalita H. Selective and Sensitive Detection of Formaldehyde at Room Temperature by Tin Oxide Nanoparticles/Reduced Graphene Oxide Composite. ACS Appl Nano Mater. 2023 May 12;6(9):7948–59. doi:10.1021/acsanm.3c01183

98. Pardeshi NM, Ghuge RS, Birla PN, Chauhan R, Bhalekar SP, Shinde MD, et al. Reduced Graphene Oxide@Bimodal TiO2 Nanocomposites as an Efficacious Console for Room Temperature n-Butanol Gas Sensing. ACS Appl Electron Mater. 2024 Jun 25;6(6):4805–18. doi:10.1021/acsaelm.4c00849

99. Zito CA, Perfecto TM, Volanti DP. Room-Temperature Triethylamine Sensor Based on Reduced Graphene Oxide/CeO2 Nanocomposites. ACS Appl Nano Mater. 2023 May 26;6(10):9041–9. doi:10.1021/acsanm.3c01734

100. Zhao C, Fu H, He P, Bai Y, Chen F, Shi N, et al. Room-temperature sensing performance of CuO/Cu2O nanocomposites towards n-butanol. Sens Actuators B Chem. 2022 Dec 15;373. doi:10.1016/j.snb.2022.132630

101. Zhang S, Song P, Zheng Y, Ding Y, Wang Q. MoO2/MoO3/MXene ternary nanocomposites for high-performance ethanol detection at room temperature. J Alloys Compd. 2022 Dec 5;925. doi:10.1016/j.jallcom.2022.166663

102. Krishna KG, Parne SR, Nagaraju P. An optical study of heterojunction n-ZnO/p-CuO nanosheets and detection of n-butanol vapour at room temperature. J Mater Sci. 2023 Oct 1;58(40):15660–75. doi:10.1007/s10853-023-08997-0

103. Khan FU, Mehmood S, Liu S, Xu W, Shah MN, Zhao X, et al. A p-n Heterojunction Based Pd/PdO@ZnO Organic Frameworks for High-Sensitivity Room-Temperature Formaldehyde Gas Sensor. Front Chem. 2021 Sep 20;9. doi:10.3389/fchem.2021.742488

104. Bhowmik B, Chowdhury NK, Guha PK, Singh AK. Room temperature selective propanol sensor based on p-TiO2 NP /n-ZnO NS heterojunction interfaces. Materials Science and Engineering: B. 2025 Aug 1;318. doi:10.1016/j.mseb.2025.118295

105. Zhang L, Kang Y, Tang Y, Yu F. UV-Activated ZnO–NiO heterojunction sensor for ethanol gas detection at low working temperature. Mater Sci Semicond Process. 2024 Jan 1;169. doi:10.1016/j.mssp.2023.107925

106. Guo L, Liang H, Hu H, Shi S, Wang C, Lv S, et al. Large-Area and Visible-Light-Driven Heterojunctions of In2O3/Graphene Built for ppb-Level Formaldehyde Detection at Room Temperature. ACS Appl Mater Interfaces. 2023;15(14). doi:10.1021/acsami.3c00218

107. Ponnusamy KM, Ghuge RS, Raveendran N, Satheesh PP, Durairaj S, Eswaran SK, et al. Vertical MoS2 Nanosheets via Space-Confined CVD for Room Temperature Photo-Enhanced Highly Selective Triethylamine Sensing. ACS Appl Nano Mater. 2024;7(6). doi:10.1021/acsanm.4c00697

108. Ghuge RS, Reji RP, Jayaraman SV, Sivalingam Y. Combinatorial Scanning Kelvin Probe and Density Functional Theory Studies on Selective n-Butanol Adsorption Properties of pH-Dependent Bi2WO6 Nanostructures. ACS Appl Electron Mater. 2024. doi:10.1021/acsaelm.4c00773

109. George J, Vikraman HK, Ghuge RS, Reji RP, Jayaraman SV, Magna G, et al. Self-Powered, Photovoltaic-Driven NH_3 Sensor: Ultra-High Selectivity, High Sensitivity, and IoT-Enabled Real-Time Monitoring with Novel Organic Molecule Functionalized TiZnN2/p-Si Heterostructure. Small. 2025;21(26). doi:10.1002/smll.202502324

110. Xu F, Ho HP. Light-activated metal oxide gas sensors: A review. Micromachines. MDPI AG; 2017. doi:10.3390/mi8110333

111. Lee J, Kim M, Park S, Ahn J, Kim ID. Materials Engineering for Light-Activated Gas Sensors: Insights, Advances, and Future Perspectives. Advanced Materials. 2025. doi:10.1002/adma.202508204

112. Weyrauch I, Hefler EL, Breuch R, Kaul P, Mathur S, Konstantynovski K. Recent Developments in the Design of Photoactivated Metal Oxide Gas Sensors and Application of Plasmonic Nanoparticles in Hydrogen-Sensing Devices. Physica Status Solidi (A) Applications and Materials Science. 2025. doi:10.1002/pssa.202400633

113. He H, Zhao C, Xu J, Qu K, Jiang Z, Gao Z, et al. Exploiting Free-Standing p-CuO/n-TiO2 Nanochannels as a Flexible Gas Sensor with High Sensitivity for H2S at Room Temperature. ACS Sens. 2021 Sep 24;6(9):3387–97. doi:10.1021/acssensors.1c01256 PubMed PMID: 34464096.

114. Zhang L, Kang Y, Tang Y, Yu F. UV-Activated ZnO–NiO heterojunction sensor for ethanol gas detection at low working temperature. Mater Sci Semicond Process. 2024;169. doi:10.1016/j.mssp.2023.107925

115. Pargoletti E, Hossain UH, Di Bernardo I, Chen H, Tran-Phu T, Chiarello GL, et al. Engineering of SnO2-Graphene Oxide Nanoheterojunctions for Selective Room-Temperature Chemical Sensing and Optoelectronic Devices. ACS Appl Mater Interfaces. 2020 Sep 2;12(35):39549–60. doi:10.1021/acsami.0c09178 PubMed PMID: 32696650.

116. Sun Y, Cui J, Fu S, Sun S, Qian K, Luo Z, et al. Rare Earth-Driven Photogenerated Charge Separation in SnO2@Y2O3 Heterojunctions for Enhanced H2S Sensing at Room Temperature. ACS Appl Mater Interfaces. 2025 Mar 12;17(10):15948–58. doi:10.1021/acsami.4c19811 PubMed PMID: 40016912.

117. You J, Zhu Y, Wang D, Li J, Liang Y, Yang Y, et al. Enhanced S-scheme mechanism in sandwich-type NiO/Ag/ZnIn2S4 heterojunction nanoarray for room temperature triethylamine sensing under visible light excitation. Talanta. 2025 Dec 1;295. doi:10.1016/j.talanta.2025.128378 PubMed PMID: 40424791.

118. Suh JM, Eom TH, Cho SH, Kim T, Jang HW. Light-activated gas sensing: A perspective of integration with micro-LEDs and plasmonic nanoparticles. Materials Advances. Royal Society of Chemistry; 2021. p. 827–44. doi:10.1039/d0ma00685h

119. Nasriddinov A, Zairov R, Rumyantseva M. Light-activated semiconductor gas sensors: pathways to improve sensitivity and reduce energy consumption. Front Chem. 2025;Volume 13-2025. doi:10.3389/fchem.2025.1538217

120. Ghuge RS, Madhavanunni Rekha S, Vikraman HK, Velappa Jayaraman S, Kiran MSRN, Bhat SV, et al. Transparent TiO2/MoO3 Heterojunction-Based Photovoltaic Self-Powered Triethylamine Gas Sensor with IoT-Enabled Smartphone Interface. ACS Sens. 2024 Dec 27;9(12):6592–604. doi:10.1021/acssensors.4c02110 PubMed PMID: 39591497.

121. Li L, Zhou L, Hu Z, Li T, Chen B, Li HY, et al. Hollow-Out Fe2O3-Loaded NiO Heterojunction Nanorods Enable Real-Time Exhaled Ethanol Monitoring under High Humidity. ACS Appl Mater Interfaces. 2023 Mar 29;15(12):15707–20. doi:10.1021/acsami.2c23088 PubMed PMID: 36924356.

122. Cheng W, Li X, Han C, Liu Y, Xue A, Dong H, et al. Room-Temperature Wearable Chemiresistor Based on a Flexible Inorganic Photoactive Anatase-Rutile TiO2/Yttria-Stabilized Zirconia Nanofiber Network. ACS Sens. 2025 Mar 28;10(3):2125–35. doi:10.1021/acssensors.4c03380 PubMed PMID: 40063984.

123. Ma Z, Wang Z, Gao L. Light-Assisted Enhancement of Gas Sensing Property for Micro-Nanostructure Electronic Device: A Mini Review. Frontiers in Chemistry. 2021. doi:10.3389/fchem.2021.811074

124. Chen H, Chen H, Chen J, Song M. Gas Sensors Based on Semiconductor Metal Oxides Fabricated by Electrospinning: A Review. Sensors. 2024. doi:10.3390/s24102962

125. Jamalzadegan S, Xu J, Shen Y, Mativenga B, Li M, Zare M, et al. Advancing Wearable VOC Sensors: A Roadmap for Sustainable Agriculture and Real-Time Plant Health Monitoring. Chem and Bio Engineering. American Chemical Society; 2025. doi:10.1021/cbe.5c00027

126. Zhao L, Chen Y, Li X, Li X, Lin S, Li T, et al. Room temperature formaldehyde sensing of hollow sno2/zno heterojunctions under uv-led activation. IEEE Sens J. 2019 Sep 1;19(17):7207–14. doi:10.1109/JSEN.2019.2916879

127. Rekha SM, Ghuge RS, Vikraman HK, Kiran MSRN, Sivalingam Y, Bhat SV. ZnO/CuI Heterojunction UV-Photovoltaic Gas Sensor for Self-Powered IoT-Integrated n-Butylamine VOC Detection. Adv Mater Technol. 2025;10(15). doi:10.1002/admt.202500456

128. Zhang J, Shen H, Li Y, Wang L, Xie ZH, Chen A, et al. Room temperature acetone gas sensor based on B-TiO2/CuS heterojunction utilizing visible light activation. Ceram Int. 2025;51(26). doi:10.1016/j.ceramint.2025.08.272

129. Li J, Gu D, Yang Y, Du H, Li X. UV Light Activated SnO2/ZnO Nanofibers for Gas Sensing at Room Temperature. Front Mater. 2019;6. doi:10.3389/fmats.2019.00158

130. Chang HK, Ko DS, Cho DH, Kim S, Lee HN, Lee HS, et al. Enhanced response of the photoactive gas sensor on formaldehyde using porous SnO2@TiO2 heterostructure driven by gas-flow thermal evaporation and atomic layer deposition. Ceram Int. 2021;47(5). doi:10.1016/j.ceramint.2020.10.172

131. Chang X, Qiao X, Li K, Wang P, Xiong Y, Li X, et al. UV assisted ppb-level acetone detection based on hollow ZnO/MoS2 nanosheets core/shell heterostructures at low temperature. Sens Actuators B Chem. 2020;317. doi:10.1016/j.snb.2020.128208

132. Bagheri F, Haratizadeh H, Afzali S. Selective sensing of triethylamine (TEA) using Zn2SnO4-SnO2 nanocomposites under UV irradiation at room temperature. Sens Actuators A Phys. 2025 Sep 1;391. doi:10.1016/j.sna.2025.116655

133. Ling W, Zhang S, Cao S, Pu Y, Zhu D. Enhanced acetic acid detection for Tb2O3 @MOF-derived ZnO at room temperature. Sens Actuators B Chem. 2023;377. doi:10.1016/j.snb.2022.133057

134. Guo L, Liang H, Hu H, Shi S, Wang C, Lv S, et al. Large-Area and Visible-Light-Driven Heterojunctions of In2O3/Graphene Built for ppb-Level Formaldehyde Detection at Room Temperature. ACS Appl Mater Interfaces. 2023 Apr 12;15(14):18205–16. doi:10.1021/acsami.3c00218 PubMed PMID: 36999948.

135. Han L, Wang D, Cui J, Chen L, Jiang T, Lin Y. Study on formaldehyde gas-sensing of In 2O 3-sensitized ZnO nanoflowers under visible light irradiation at room temperature. J Mater Chem. 2012 Jul 7;22(25):12915–20. doi:10.1039/c2jm16105b

136. Nam GB, Ko J, Choi S, Choi S, Yang JW, Kwon HR, et al. Visible Light-Driven Heterojunction Array Based on Type-I In2S3/In2O3 for Selective Multi-Gas Discrimination. Small. 2026;22(1). doi:10.1002/smll.202506056

137. Abdelghani RM, Kashyout AEHB, Morsi I, Taha TE, Soliman NF, El-Shafai W. Synthesis and characterization of hematite nanomaterials imprinted with acetone, ethanol and methanol for AI-Based IoT gas sensor arrays. Sci Rep. 2025 Dec 1;15(1). doi:10.1038/s41598-025-06724-0 PubMed PMID: 40813413.

138. Cai Y, Che X, Duan Y. From Volume to Mass: Transforming Volatile Organic Compound Detection with Photoionization Detectors and Machine Learning. Sensors. 2025 Sep 1;25(17). doi:10.3390/s25175314 PubMed PMID: 40942743.

139. Ramadan MNA, Ali MAH, Khoo SY, Alkhedher M, Alherbawi M. Real-time IoT-powered AI system for monitoring and forecasting of air pollution in industrial environment. Ecotoxicol Environ Saf. 2024 Sep 15;283. doi:10.1016/j.ecoenv.2024.116856 PubMed PMID: 39151373.

140. Kim D, Lee J, Park MK, Ko SH. Recent developments in wearable breath sensors for healthcare monitoring. Communications Materials. Springer Nature; 2024. doi:10.1038/s43246-024-00480-w

141. Jannat A, Talukder MMM, Li Z, Ou JZ. Recent Advances in Flexible and Wearable Gas Sensors Harnessing the Potential of 2D Materials. Small Science. 2025. doi:10.1002/smsc.202500025

142. Kim K, Chun D, Yang W. IoT-based filter management system using reinforced ANFIS for VOCs reduction in urban industrial facilities. Sci Rep. 2025 Dec 1;15(1). doi:10.1038/s41598-025-02435-8 PubMed PMID: 40394134.

No primary research results, software or code have been included and no new data were generated or analysed as part of this review.

View Article Online
DOI: 10.1039/D6NA00239K